Non Linear Evolution of Acoustic Oscillations

Roman Scoccimarro (NYU)

Renormalized Cosmological Perturbation Theory

Crocce and Scoccimarro, astro-ph/0509418-9, + in preparation

The scale dependence of halo and galaxy bias

Smith, Sheth and Scoccimarro, in preparation

Extracting cosmological information requires understanding of nonlinearities

- Knowledge of the transition to the nonlinear regime helps significantly in constraining the growth factor and therefore e.g. constraints dark energy or modifications of general relativity.

- Studies of baryon acoustic oscillations imprinted on the dark matter power spectrum can be used to determine the angular diameter distance, which constraints the expansion history of the universe. However, these acoustic signatures are modified by weakly nonlinear evolution.

- Nonlinearities play an important role in the determination of cosmological parameters from large-scale structure surveys. Our inability to model them accurately puts a limit to the cosmological information we can extract.

Standard Perturbative Approach to Gravitational Clustering

- The Universe is homogeneous at large (Hubble) scales. Fluctuations become larger as small scales are approached.

- In standard perturbation theory (PT), one expands in the amplitude of density perturbations.

- This is well justified when looking for asymptotic behavior at large-scales, where fluctuations become small. PT at these scales is successful in predicting N-point correlation functions.

- In diagrammatic language, where a given topology uniquely describes the size of contributions in terms of the amplitude of fluctuations, such calculations are obtained by "tree" diagrams.

- How about nonlinear corrections (corresponding to "one-loop" diagrams) to tree-level results?

- Once these become important, one basically needs to sum up all orders in PT (i.e. number of loops) to obtain meaningful answers, since the expansion parameter becomes of order unity or larger.

- For the power spectrum (N=2), taking into account just one-loop corrections to the linear spectrum works well for steep spectra but not so well for CDM spectra at z=0.

- Similar results hold for the bispectrum (N=3).

Why not just use N-Body simulations?

Simulations are extremely useful and rely on approximations that do not assume small fluctuations. However, there are benefits in having a complementary approach:

- Successful comparison reinforces validity of both, and differences lead to understanding of limitations of one method over another.

- Interplay between simulations and analytic results (e.g. as in fitting formulae)

- Physical insight and understanding of details difficult to extract from complex simulations.

- Computational cost is large for scanning over cosmological parameter space.

- Simulations make truncations of dynamics: finite box size and particle number, generation of initial conditions.

- Accuracy required for future observations are still far from being realized in simulations, e.g. comparison between different codes with identical initial conditions show significant differences for the dark matter power spectrum:

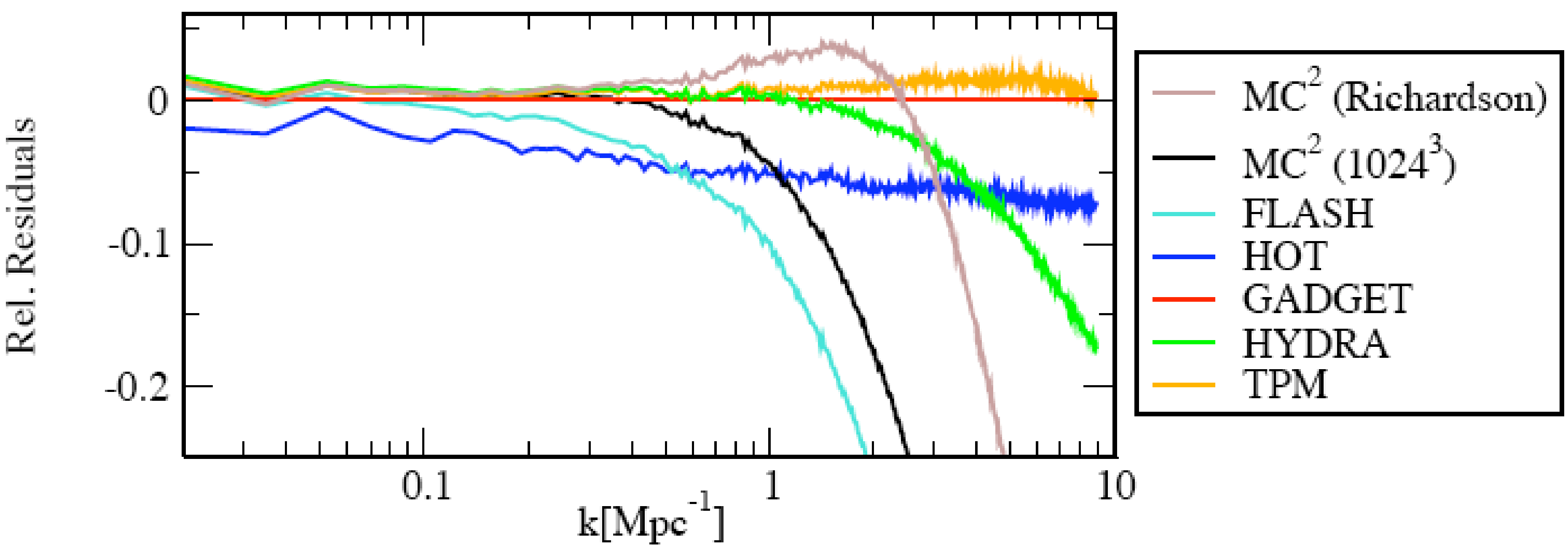

Heitmann et al. (2005)

Renormalized Perturbation Theory (RPT)

- In RPT, one looks at the infinite series of diagrams in PT for correlation functions and sees how they organize themselves into a few characteristic physical quantities, the most important of which is the propagator

Final density / velocity div.

$$G_{ab}(k,\eta)\ \delta_{\rm D}(\mathbf{k}-\mathbf{k}') \equiv \left\langle \frac{\delta\Psi_a(\mathbf{k},\eta)}{\delta\phi_b(\mathbf{k}')} \right\rangle$$

Initial Conditions

where

$$\Psi_a(\mathbf{k},\eta) \equiv \Big(\delta(\mathbf{k},\eta),\ -\theta(\mathbf{k},\eta)/\mathcal{H}\Big), \qquad \eta \equiv \ln a(\tau).$$

$$\phi_a(\mathbf{k}) = \Psi_a(\mathbf{k},\eta=0)$$

Equations of motion can be written as,

$$\partial_\eta \Psi_a(\mathbf{k},\eta) + \Omega_{ab}\Psi_b(\mathbf{k},\eta) = \gamma_{abc}(\mathbf{k},\mathbf{k}_1,\mathbf{k}_2)\Psi_b(\mathbf{k}_1,\eta)\Psi_c(\mathbf{k}_2,\eta)$$

Laplace transform in time variable, $\quad (\sigma^{-1}_{ab}(\omega) \equiv \omega\delta_{ab} + \Omega_{ab})$

$$\sigma^{-1}_{ab}(\omega)\ \Psi_b(\mathbf{k},\omega) = \underset{\substack{\uparrow \\ \text{Initial Conditions}}}{\phi_a(\mathbf{k})} + \gamma^{(\mathrm{s})}_{abc}(\mathbf{k},\mathbf{k}_1,\mathbf{k}_2)\oint \frac{d\omega_1}{2\pi i}\ \Psi_b(\mathbf{k}_1,\omega_1)\Psi_c(\mathbf{k}_2,\omega-\omega_1),$$

then going back to time,

$$\Psi_a(\mathbf{k},\eta) = g_{ab}(\eta)\phi_b(\mathbf{k}) + \int_0^\eta d\eta' g_{ab}(\eta-\eta')\gamma^{(\mathrm{s})}_{bcd}(\mathbf{k},\mathbf{k}_1,\mathbf{k}_2)\Psi_c(\mathbf{k}_1,\eta')\Psi_d(\mathbf{k}_2,\eta')$$

Diagrammatically:

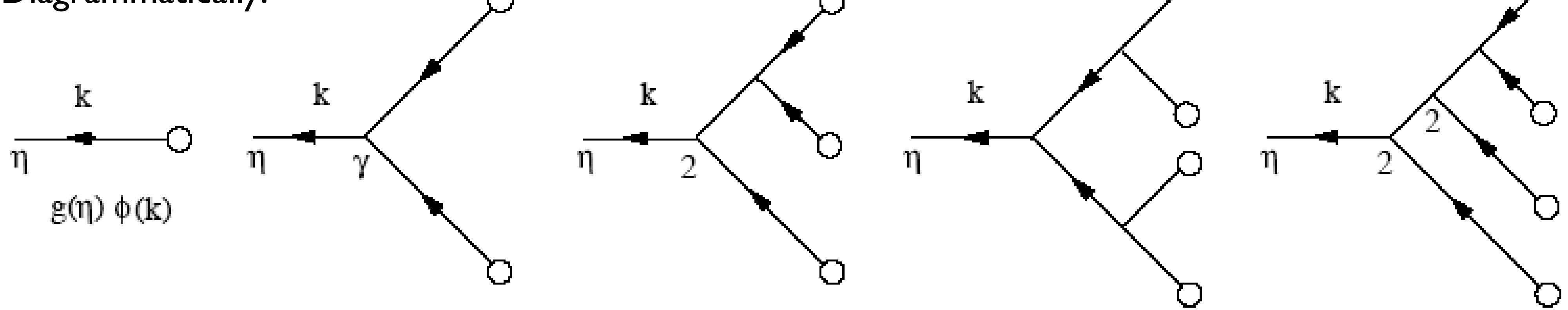

The propagator is a measure of the memory of initial conditions, and reduces to the usual growth factors in linear theory,

$$g_{ab}(\eta) = \frac{e^{\eta}}{5}\begin{bmatrix} 3 & 2 \\ 3 & 2 \end{bmatrix} - \frac{e^{-3\eta/2}}{5}\begin{bmatrix} -2 & 2 \\ 3 & -3 \end{bmatrix},$$

growing mode $\phi_a(\mathbf{k}) \propto (1, 1)$

decaying mode $\phi_a(\mathbf{k}) \propto (1, -3/2)$

At smaller scales this receives nonlinear corrections that drive the propagator to zero (the final condition "does not remember" the initial condition).

Once these terms are resummed into the nonlinear propagator, the rest of the diagrams (still an infinite number) can be thought of as the effects of mode-coupling,

- they measure generation of structure at small scales

- they dominate in a narrow range of scales, drastically improving convergence

To illustrate these ideas, let's look at the Zel'dovich approximation (particles moving in straight lines according to their primordial gravitational forces). The nonlinear power spectrum (exact, non-perturbative) in this dynamics is known,

$$P(k) = \int \frac{d^3r}{(2\pi)^3}\ \mathrm{e}^{i\mathbf{k}\cdot\mathbf{r}}\ \left[\mathrm{e}^{-[k^2\sigma_v^2 - I(\mathbf{k},\mathbf{r})]} - 1\right],$$

where,

$$I(\mathbf{k},\mathbf{r}) \equiv \int d^3q \frac{(\mathbf{k}\cdot\mathbf{q})^2}{q^4} \cos(\mathbf{q}\cdot\mathbf{r}) P_L(q), \qquad \sigma_v^2 = \frac{I(k,0)}{k^2}$$

Let's now expand this result in powers of the linear spectrum, to recover the standard PT expansion,

$$P(k) = \int \frac{d^3r}{(2\pi)^3}\ \mathrm{e}^{i\mathbf{k}\cdot\mathbf{r}}\ \sum_{n=1}^{\infty} \frac{(-1)^n}{n!}[k^2\sigma_v^2 - I(\mathbf{k},\mathbf{r})]^n \equiv \sum_{\ell=0}^{\infty}\ P_{\mathrm{PT}}^{(\ell)}(k),$$

ZA Nonlinear Power Spectrum in standard PT expansion

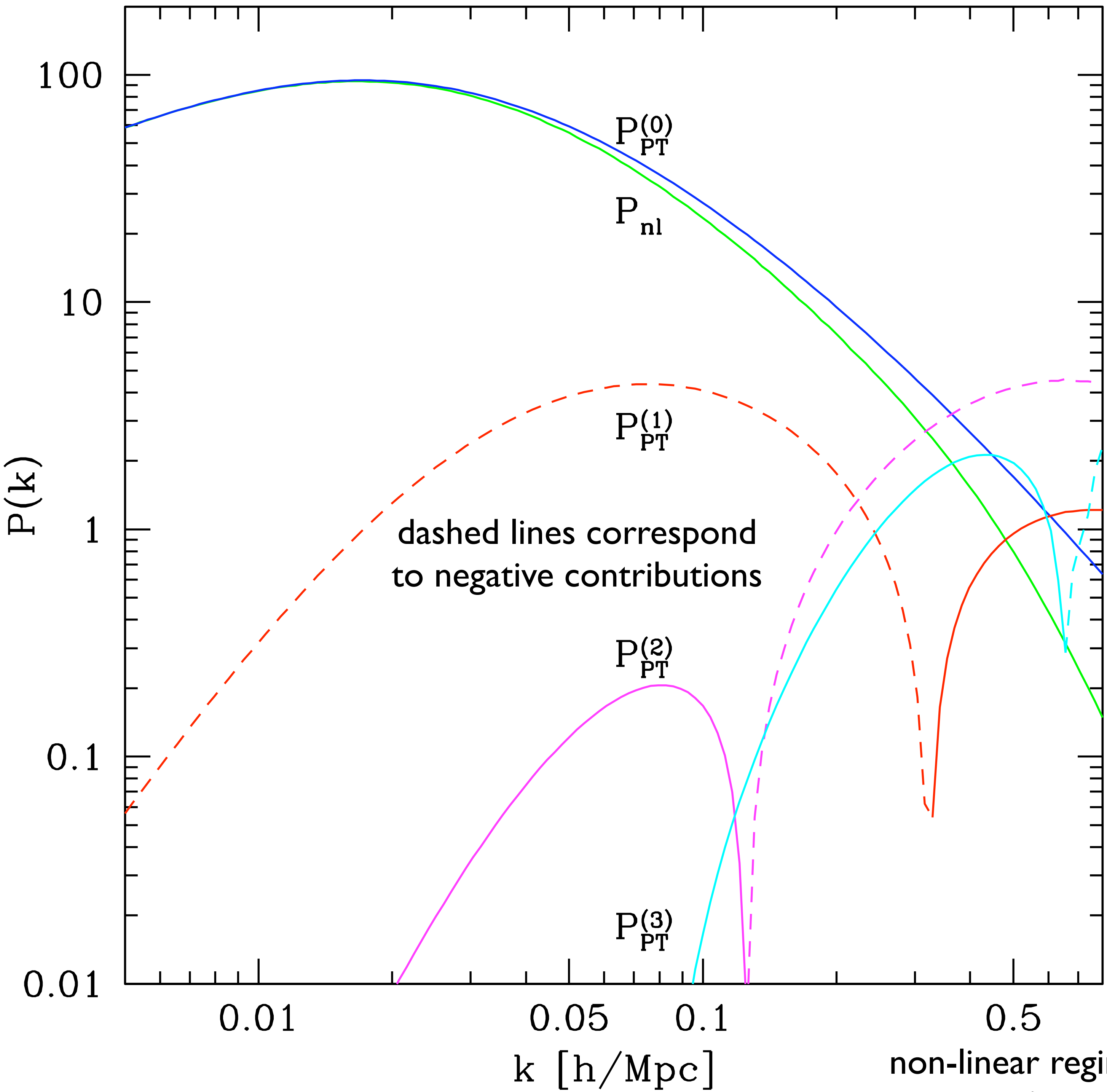

Different orders become comparable in the nonlinear regime

non-linear regime

Now, it can be shown that in RPT the resummation of the terms that represent the nonlinear propagator leads to the first exponential factor in the exact result

$$P(k) = \int \frac{d^3r}{(2\pi)^3}\, e^{i\mathbf{k}\cdot\mathbf{r}} \left[e^{-[k^2\sigma_v^2 - I(\mathbf{k},\mathbf{r})]} - 1 \right],$$

And the RPT expansion corresponds to expanding only the terms with I,

$$P(k) = \int \frac{d^3r}{(2\pi)^3}\, e^{i\mathbf{k}\cdot\mathbf{r}}\, e^{-k^2\sigma_v^2} \sum_{n=1}^{\infty} \frac{[I(\mathbf{k},\mathbf{r})]^n}{n!} \equiv \sum_{\ell=0}^{\infty} P_{\mathrm{RPT}}^{(\ell)}(k),$$

Here the n=1 term gives the linear spectrum times the propagator resummation factor (no mode-coupling, unlike the rest of the terms)

ZA Nonlinear Power Spectrum in RPT expansion

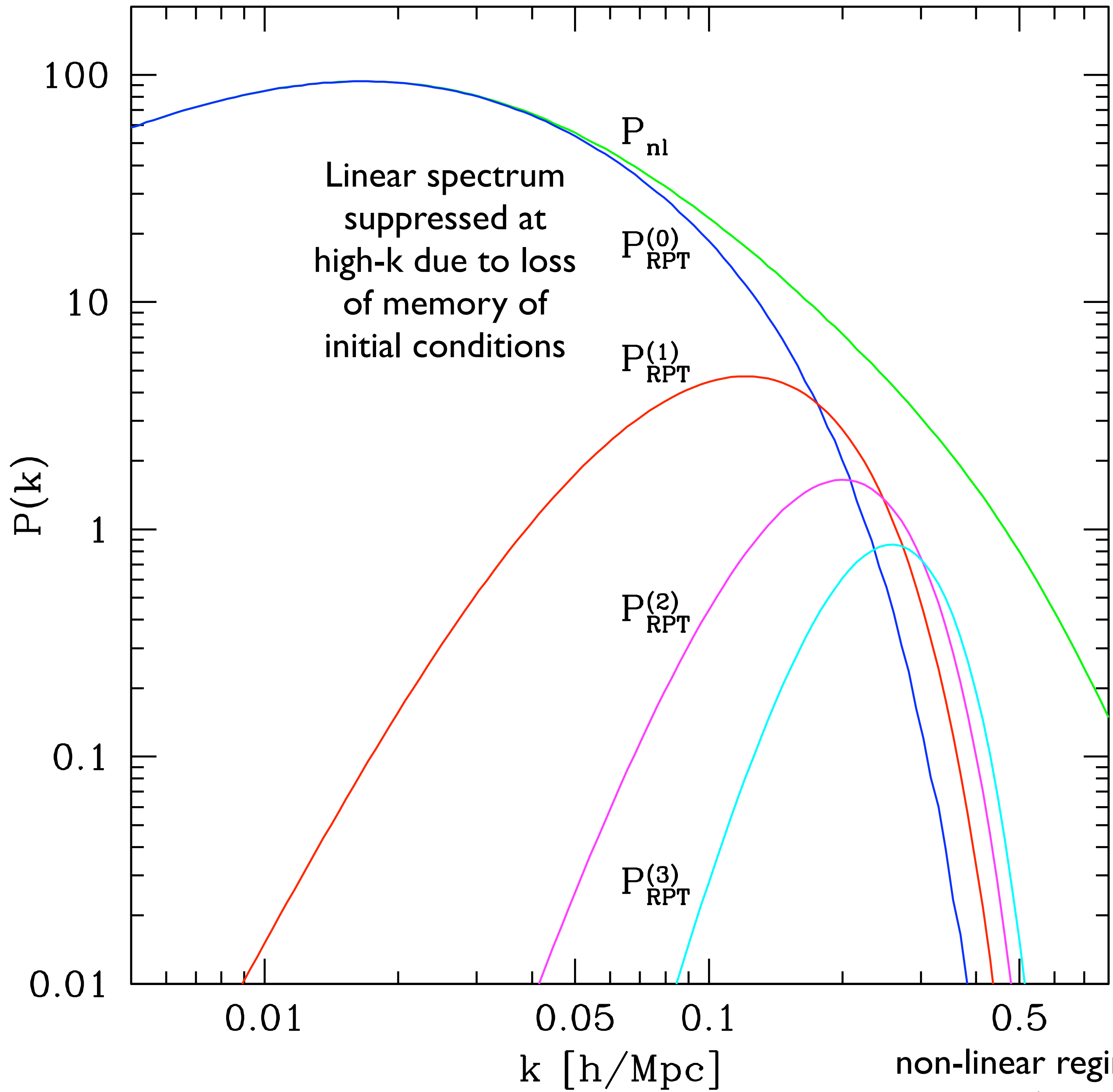

Different orders dominate only in a narrow range of scales and are always positive

non-linear regime

Measuring the Propagator from Numerical Simulations

A. From the Cross-Corrrelation:

For Gaussian initial conditions, the nonlinear propagator can be related to the cross-correlation between initial and final conditions,

$$G_{ab}(k,\eta)\,\langle\phi_b(\mathbf{k})\phi_c(\mathbf{k}')\rangle = \langle\Psi_a(\mathbf{k},\eta)\,\phi_c(\mathbf{k}')\rangle.$$

In this sense the propagator measures the memory of perturbations to their initial conditions.

B. From the Functional Derivative:

The definition involves,

$$\frac{\delta\Psi_a(\mathbf{k})}{\delta\phi_b(\mathbf{k}')} = \lim_{\epsilon\to 0}\ \frac{\Psi_a[\phi_b(\mathbf{k})+\epsilon\,\delta_{\mathrm{D}}(\mathbf{k}-\mathbf{k}')]-\Psi_a[\phi_b(\mathbf{k})]}{\epsilon}.$$

This is impractical, but doable assuming ergodicity.

Both methods give the same answer!

$$(G_\delta, G_\theta) = G_{ab}(1,1)_b = (G_{11}+G_{12}, G_{21}+G_{22})$$

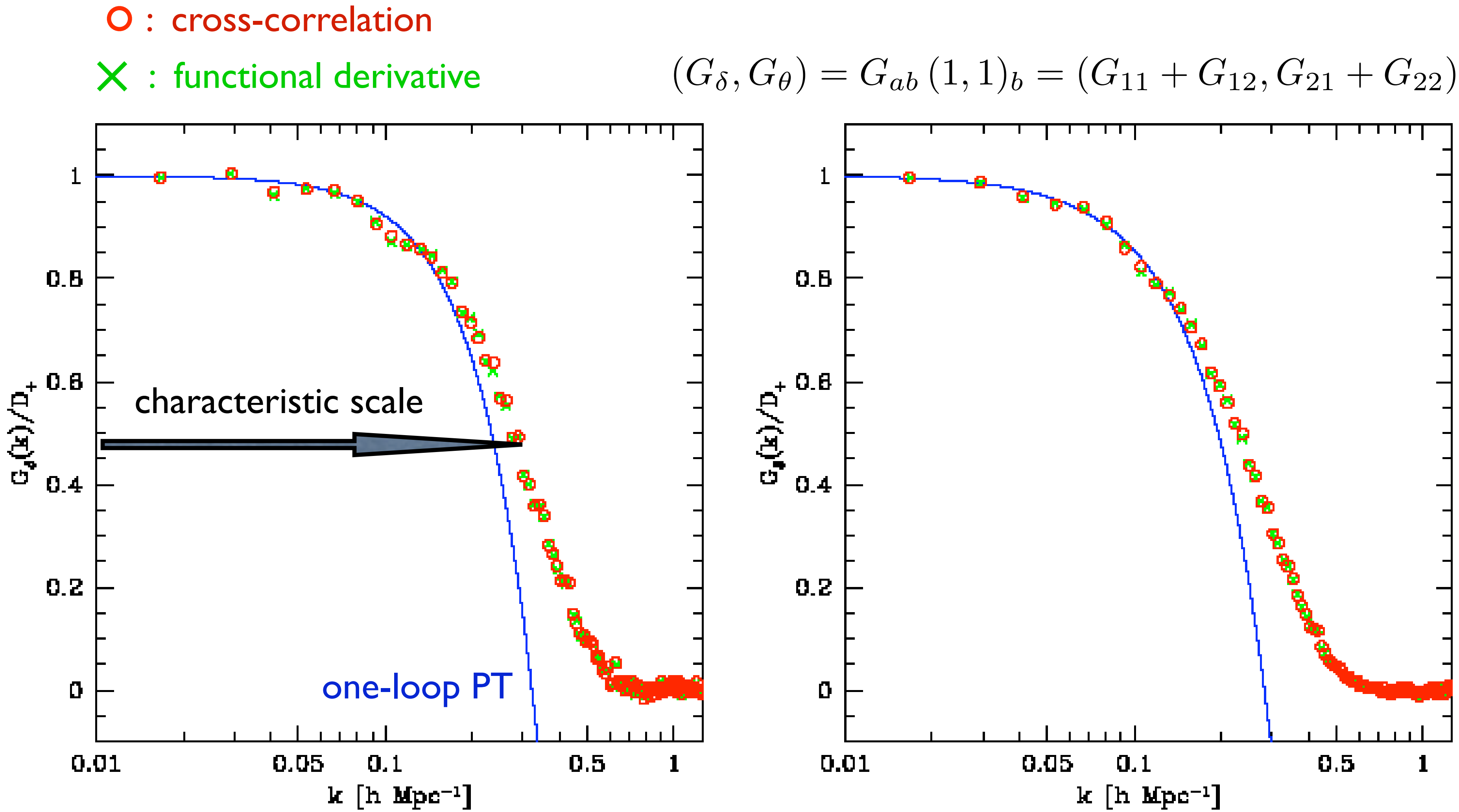

FIG. 4: The density (left panel) and velocity divergence (right panel) propagators at redshift $z = 0$ from initial conditions at $z = 5$ (corresponding to $D_+ = 4.68$). The symbols represent measurement in numerical simulations, from implementation of the functional derivative (crosses) and from the relation to the cross-correlation coefficient (circles). The solid lines show the predictions of one-loop PT, Eq. (28).

Perturbations are more non-linear than you thought...

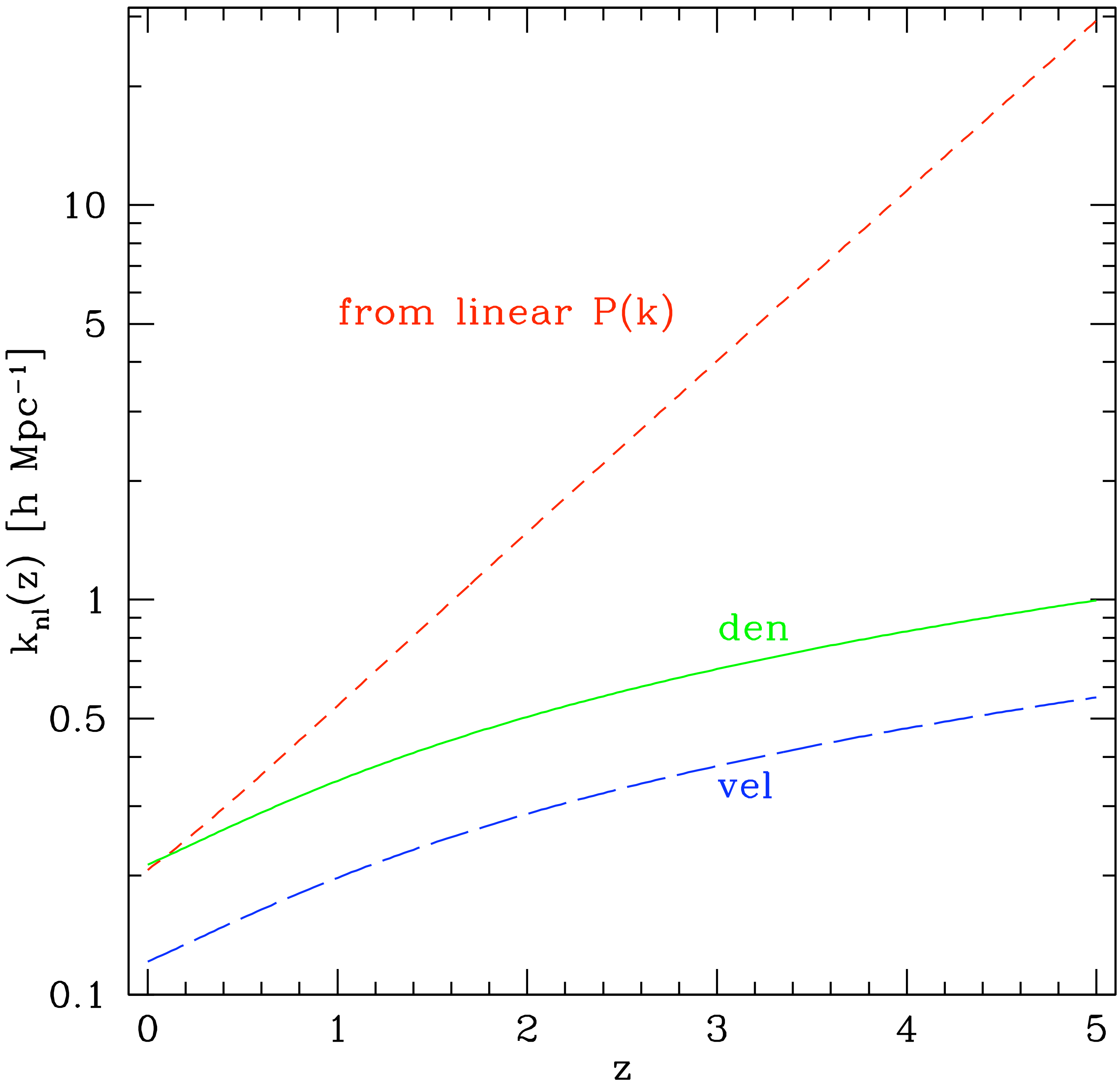

Calculating the Propagator in RPT

In the exact dynamics the resummation of the propagator can be calculated, though it is much more difficult than in ZA.

Let me just sketch how it is done.

Diagramatically, the PT expansion looks like:

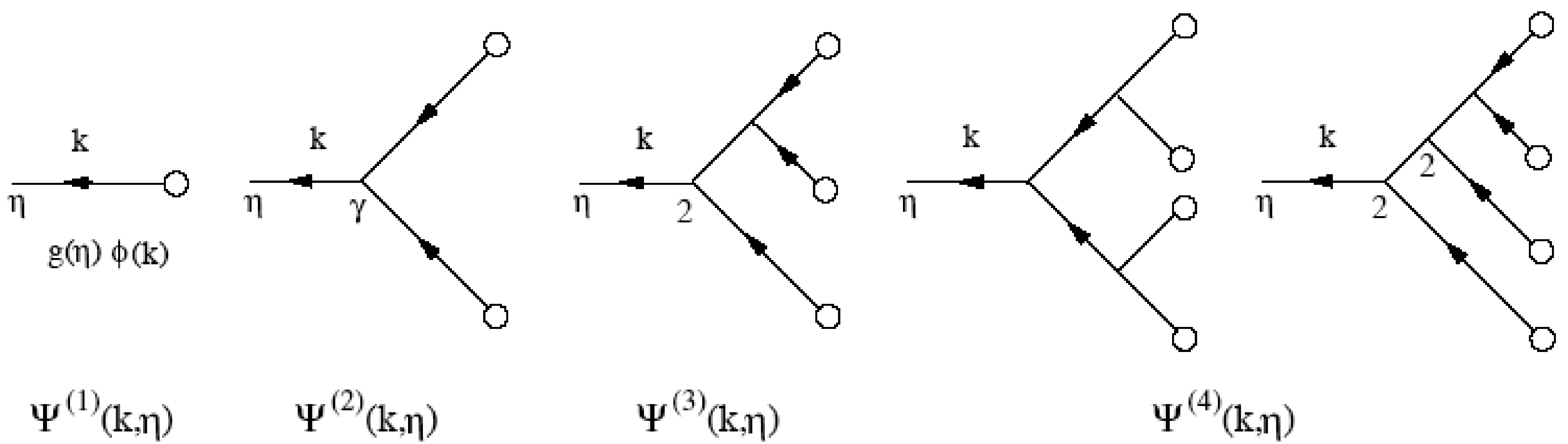

FIG. 3: Diagrams up to order $n = 4$ in the series expansion of $\Psi(\mathbf{k}, \eta)$.

Power Spectrum

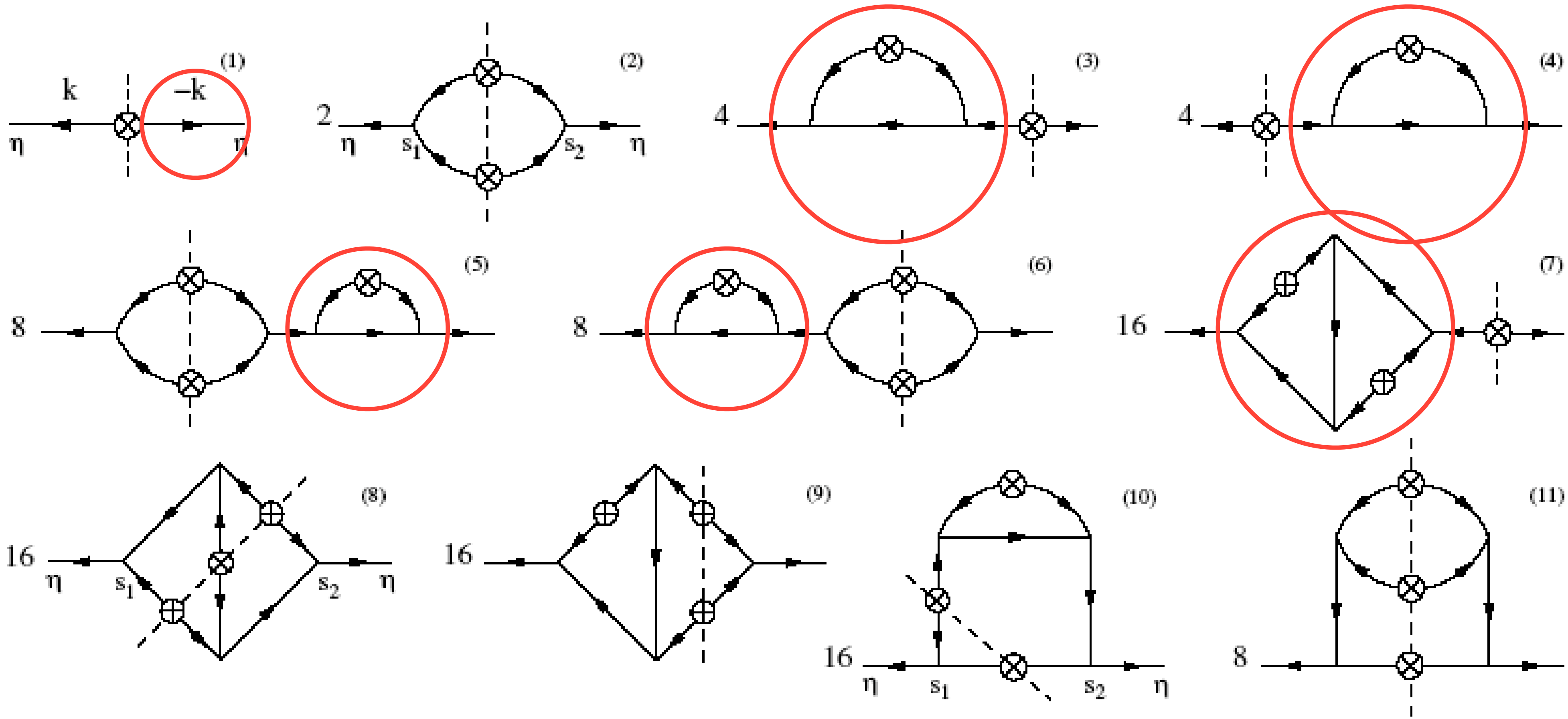

FIG. 5: Diagrams for the correlation function $P_{ab}(\mathbf{k}, \eta)$ up to two-loops (only 7 out of 29 two-loop diagrams a
hown here). The dashed lines represent the points at which the two trees representing perturbative solutions to Ψ
nd Ψ_b have been glued together.

Propagator

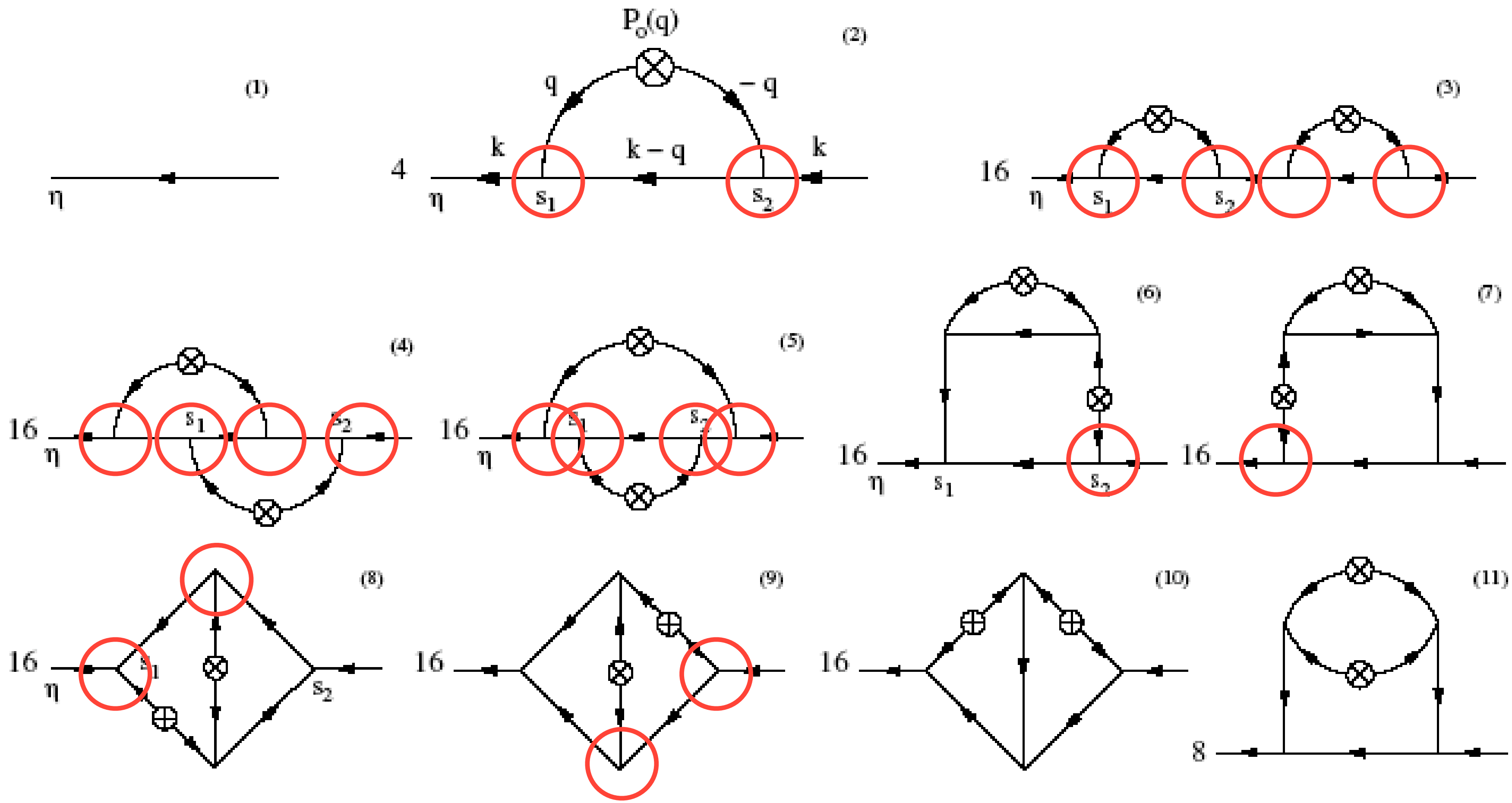

FIG. 2: Diagrams for the non linear propagator $G(k, \eta)$ up to two loops.

Let's see how the dominant contributions arise...

The dominant contributions have the *simplest* ramification possible in terms of initial conditions (that's why the cross-correlate the most):

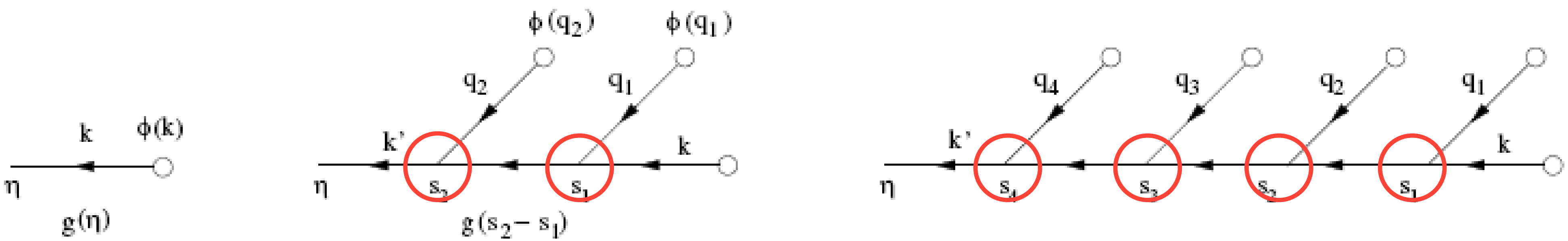

The dominant contributions can be resummed *exactly* in high-k limit!

This is so because in the high-k limit the vertex simplifies, and these diagrams have a very simple time dependence, with all propagators from initial conditions being in the purely growing mode.

These results can be extended for higher-order correlation versions of the propagator (Bernardeau, Crocce and Scoccimarro, in preparation)

$$G_{ab}(k,\eta) \simeq g_{ab}(\eta)\ \exp\Big(-\frac{1}{2}k^2\sigma_v^2(\mathrm{e}^\eta - 1)^2\Big) \qquad \text{(high-k limit)}$$

with:
$$\sigma_v^2 \equiv \frac{1}{3}\int d^3q\,\frac{P(q)}{q^2}$$

In order to recover the propagator for all scales, we match this asymptotic result to the low-k limit (one-loop correction) by

- regarding the one-loop propagator as the power series expansion of a Gaussian

and by requiring that the full propagator:

- must decay monotonically as k increases for fixed time (z).

- must decay monotonically as time increases for fixed k.

Comparison between RPT and N-Body Simulations
(z = 0, 2, 5)

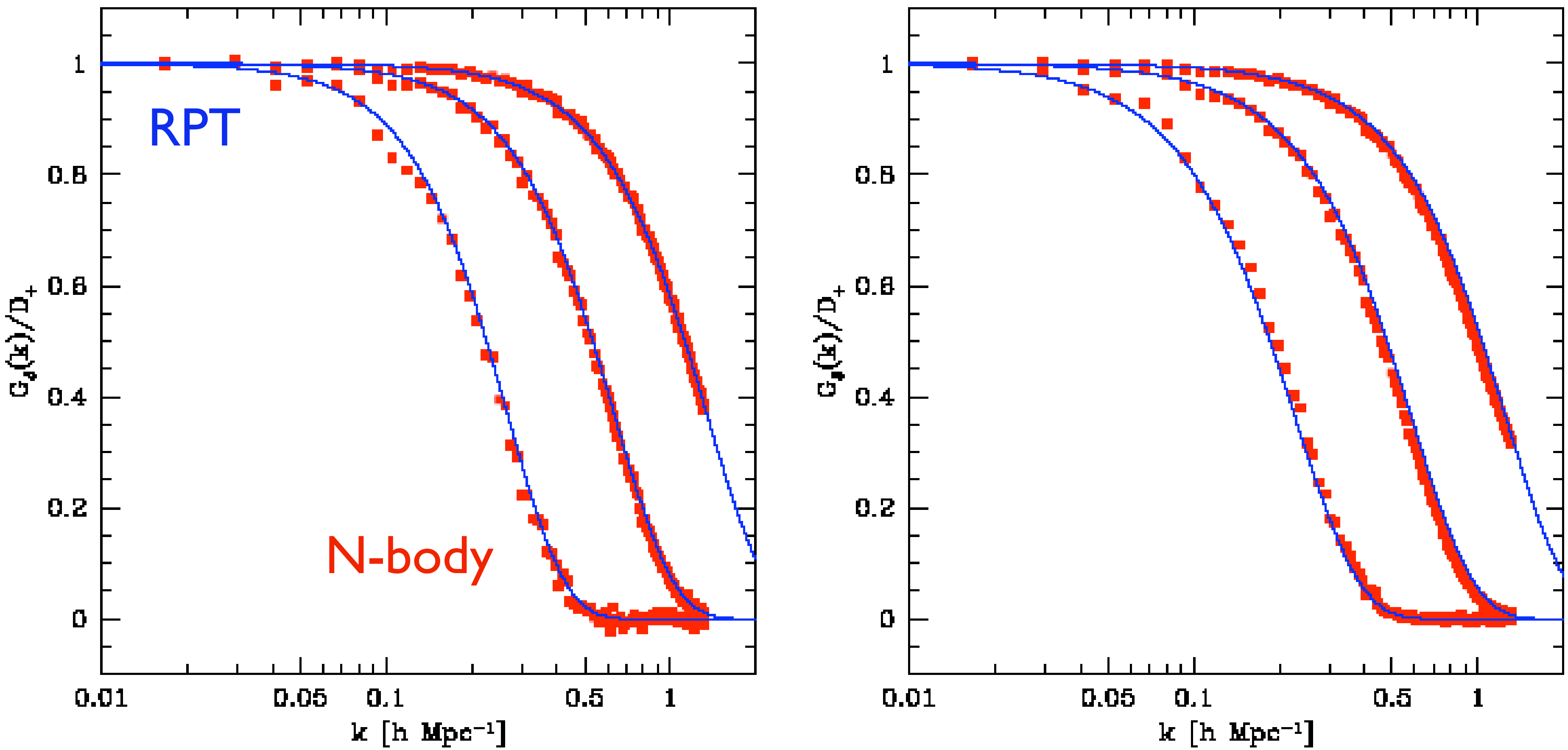

- The RPT predictions match simulations, even into the nonlinear regime, for density and velocity fields, without introducing any free parameters.

Similarities with Halo Model: P(k) is decomposed in a similar manner,

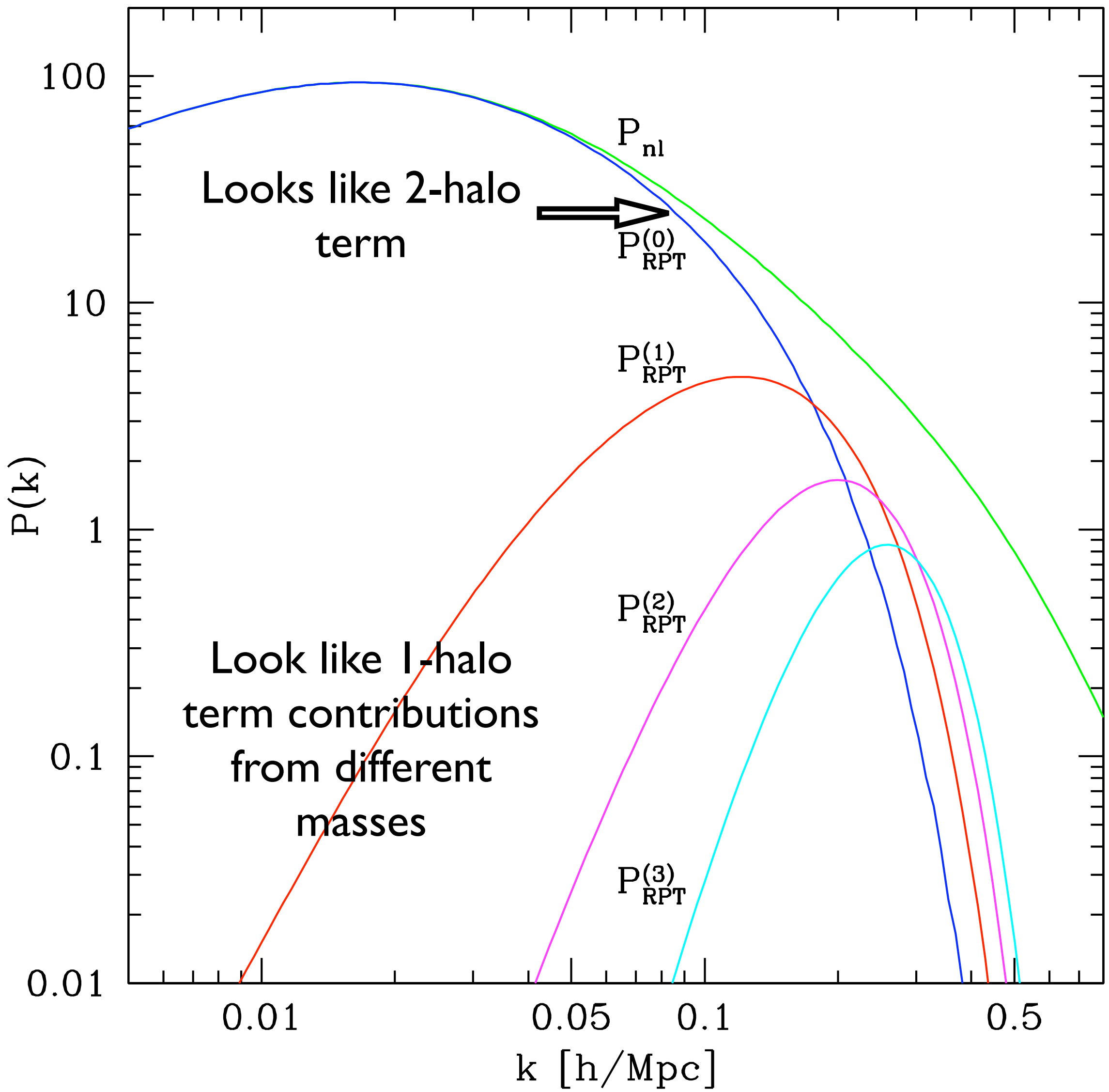

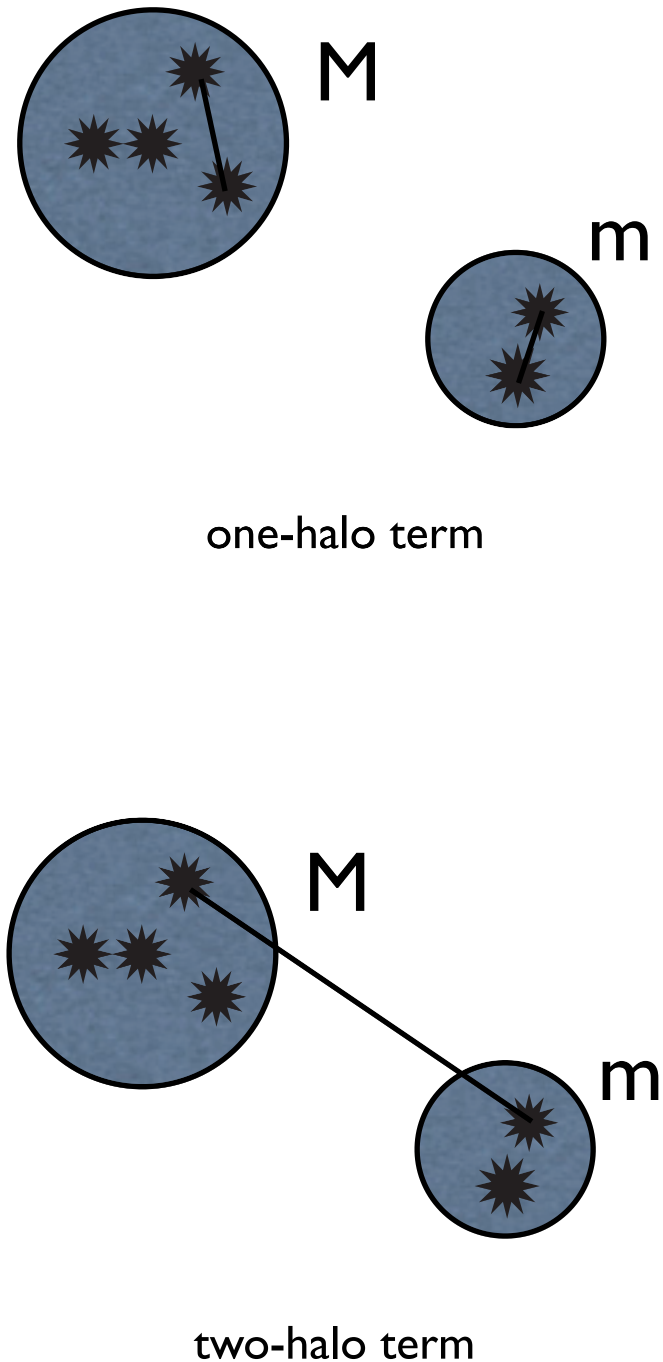

- This analogy can be made more precise. In the halo model the density is

$$\rho(\mathbf{x}) = \sum_i \underset{\substack{\uparrow \\ \text{halo masses}}}{m_i} \, \underset{\substack{\uparrow \\ \text{halo profiles}}}{u_{m_i}(\mathbf{x} - \mathbf{x}_i)}$$

Calculate the propagator in the halo model and get,

$$G_\delta(k) = \frac{D_+}{\bar{\rho}} \int m \, dm \, n(m) \, b_1(m) \; u_m(k) = D_+ \, b_1(k)$$

This gives *exactly* the form of the 2-halo term when replaced into RPT!
The 2-halo term is therefore just propagator renormalization.

A similar (though not as precise) connection can be made for the 1-halo term: in both cases these are the contributions due to mode-coupling.

Nonlinear Evolution of the Power Spectrum and Acoustic Oscillations

- Can use acoustic oscillations imprinted in the dark matter power spectrum as a probe of expansion history (to get to dark energy / modified gravity).

- This "ruler", however, gets modified due to nonlinearities

Challenge:

1% error on wiggle position induces about 8% error on w

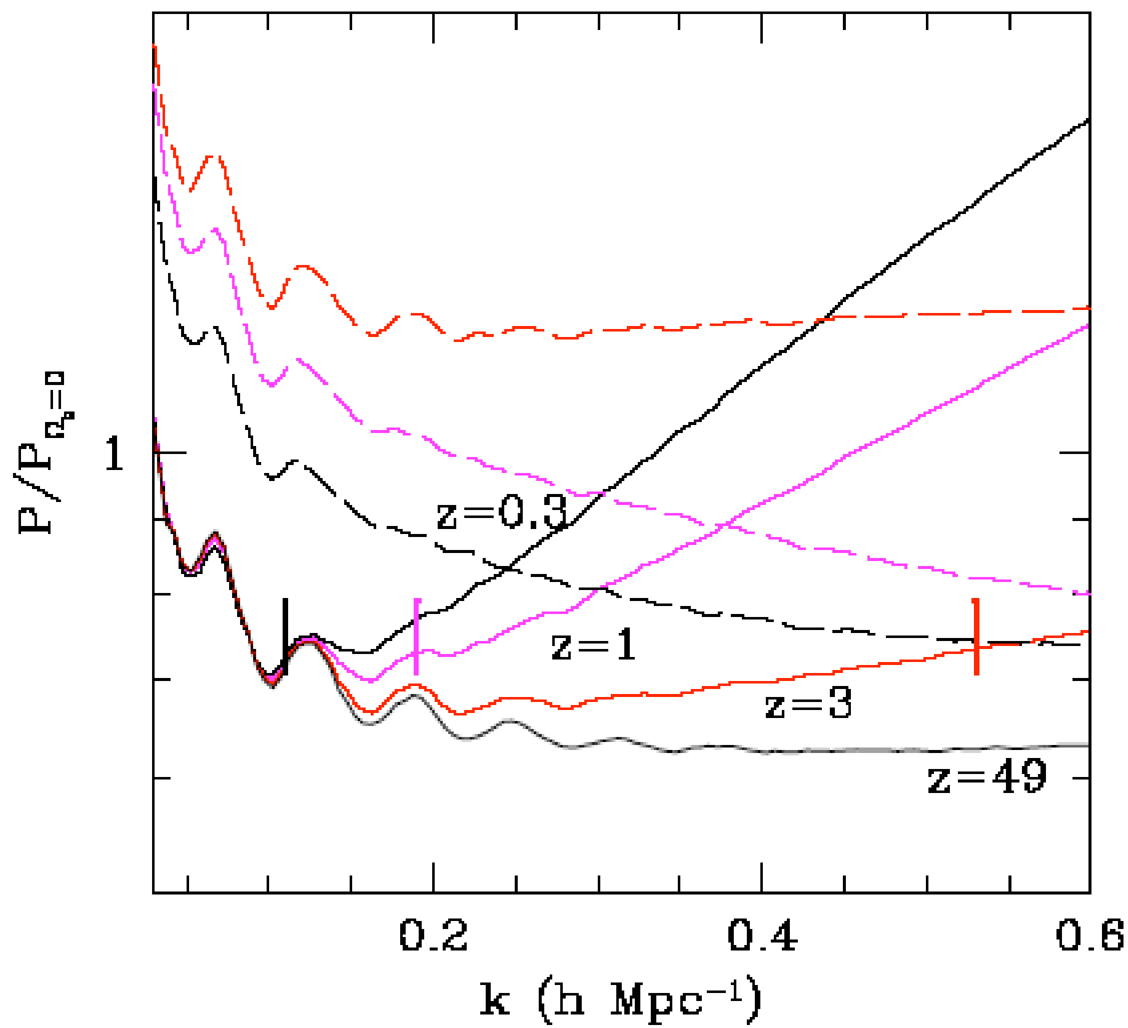

Seo & Eisenstein (2005)

This problem is somewhat challenging for simulations because,

- high resolution in Fourier space is required to resolve wiggles to the accuracy needed.

- many realizations needed to disentangle noise due to cosmic variance from true nonlinear evolution

Shortcuts are often taken,

- cosmic variance artificially suppressed by drawing initial Fourier amplitudes from their mean value (instead of random). As result the initial conditions are not Gaussian! Weak non-Gaussianity can affect nonlinear evolution.

- ratio of noisy initial conditions to expected power is used in the final condition to map the noisy final condition to a smooth answer. This mapping is only exact under linear evolution.

We want to describe the nonlinear evolution of acoustic oscillations as accurate as possible.

In order to validate RPT, we have run many realizations (8-20) of 512^3 particles in boxes 512-1024 Mpc/h a side, paying also attention to how initial conditions are generated.

The standard method used in generating initial conditions is based on the Zel'dovich approximation, which is a rather poor description of nonlinear couplings. Incorrect initial conditions at the nonlinear level generate *transients*, long-lived decaying modes that survive until low redshift.

Using second-order Lagrangian PT (2LPT) solves this problem to a large extent. These improvements become important if one is worried about percent-level accuracy in the power spectrum and mass function.

Crocce, Pueblas and Scoccimarro (2006)

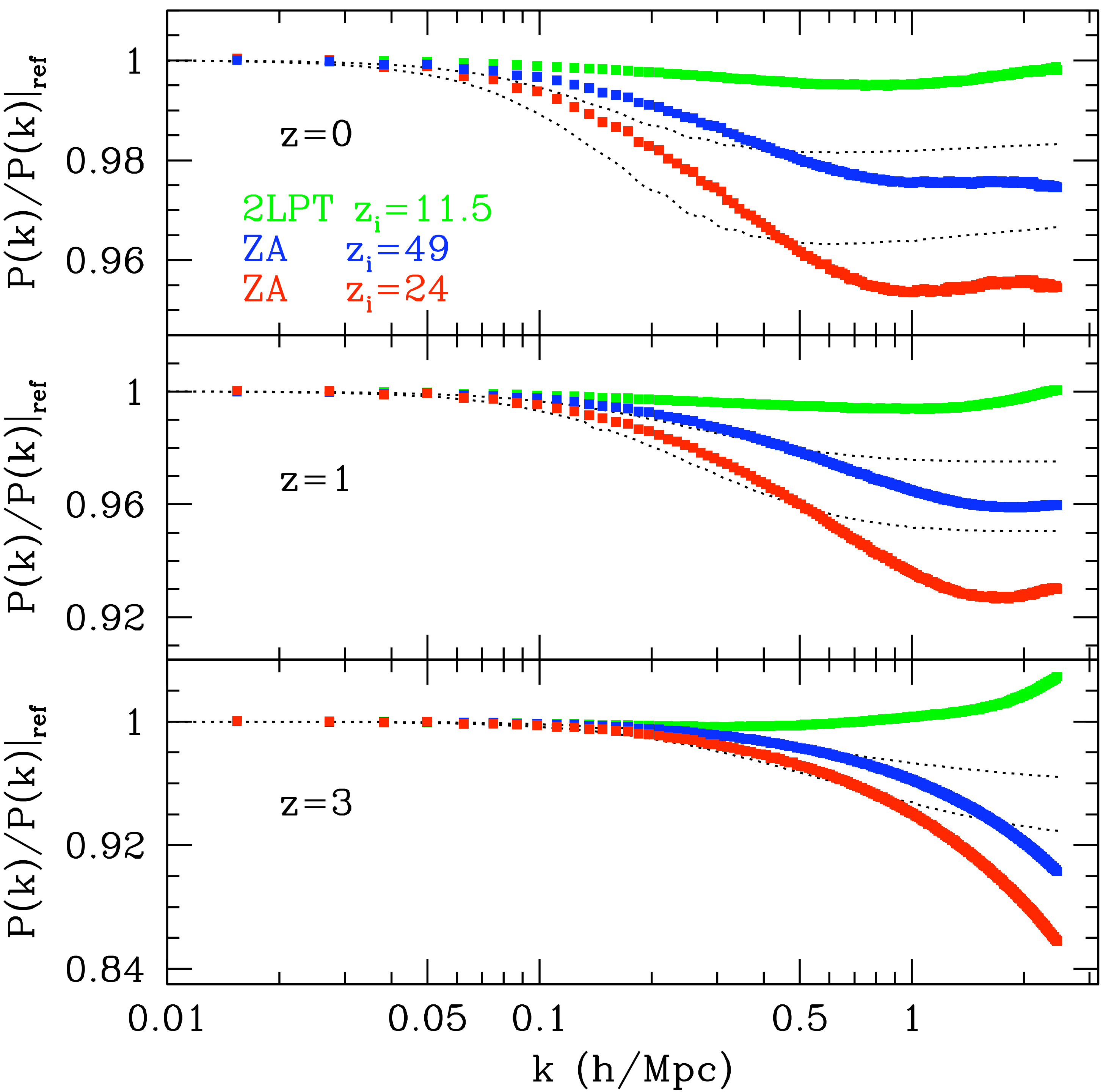

Comparison between RPT and new N-Body Simulations

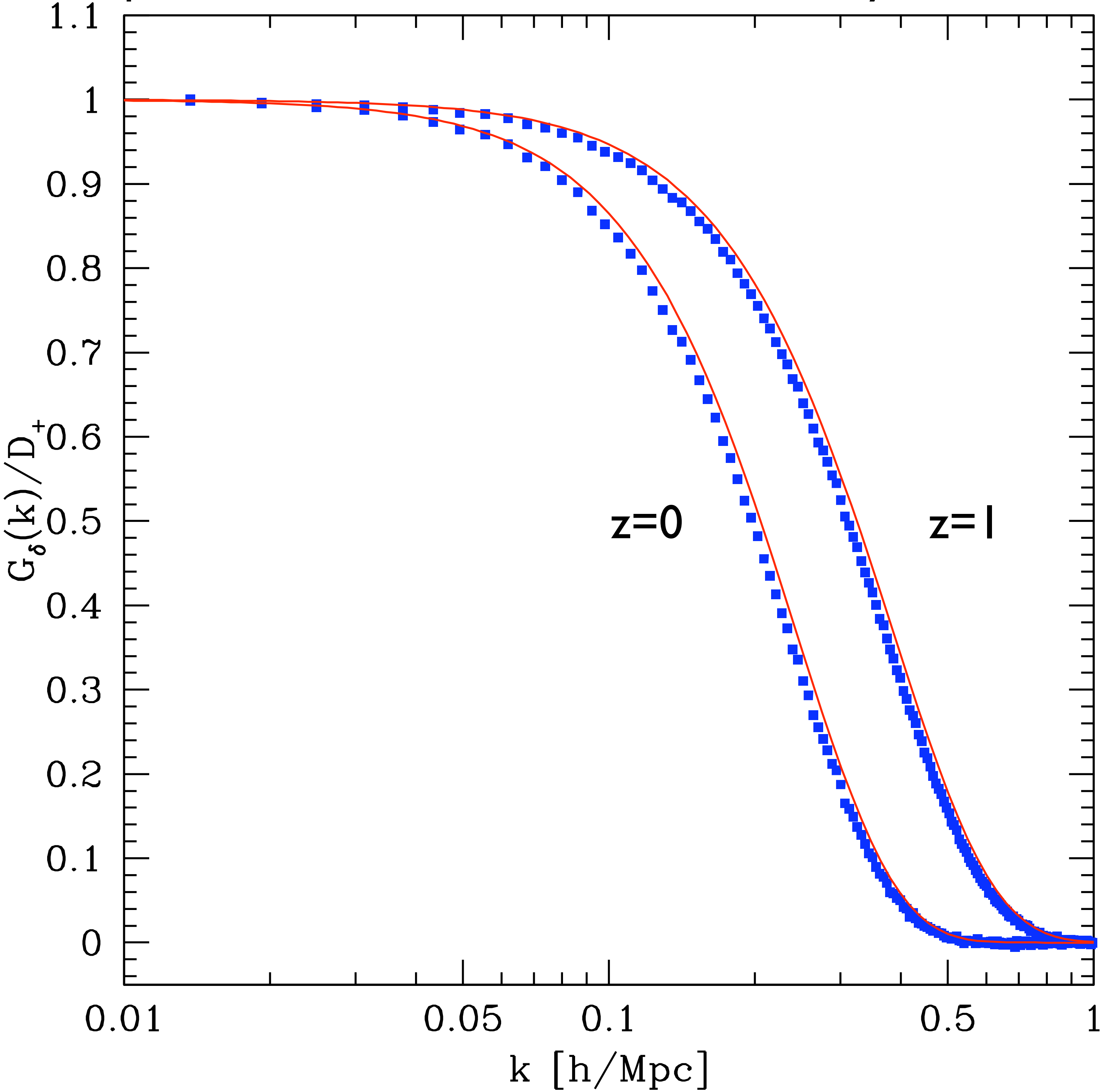

With these better simulations, we now see that RPT is slightly overestimating the propagator.

This could be due to several reasons,

1) systematics in simulations

2) sub-leading diagrams contribute slightly to the result

3) the single stream approximation (assumed in the equations of motion) is starting to break down

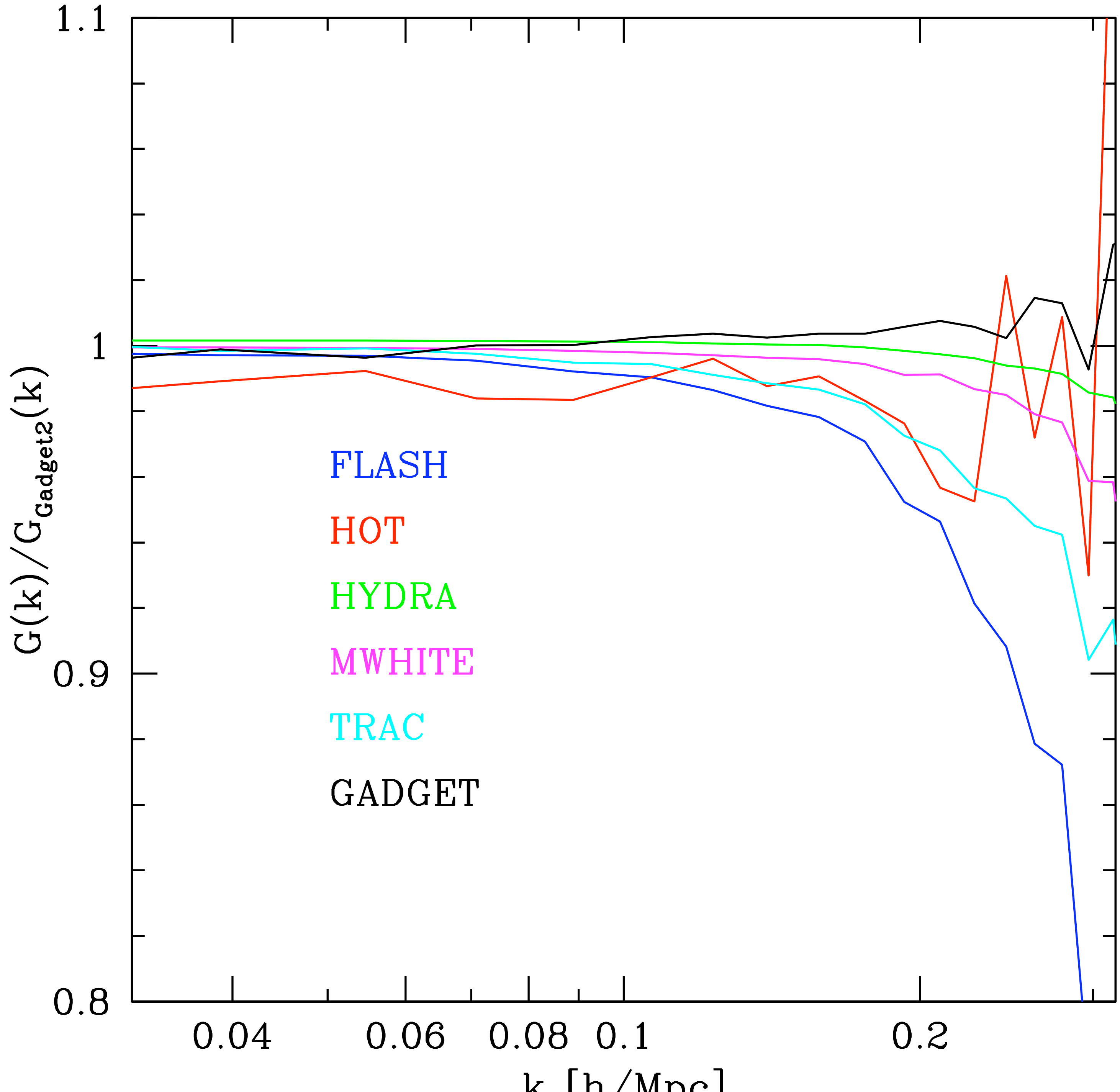
1.1
1
0.9
0.8
0.04
0.06
0.08
0.1
0.2
k [h/Mpc]
$G(k)/G_{Gadget2}(k)$
FLASH
HOT
HYDRA
MWHITE
TRAC
GADGET

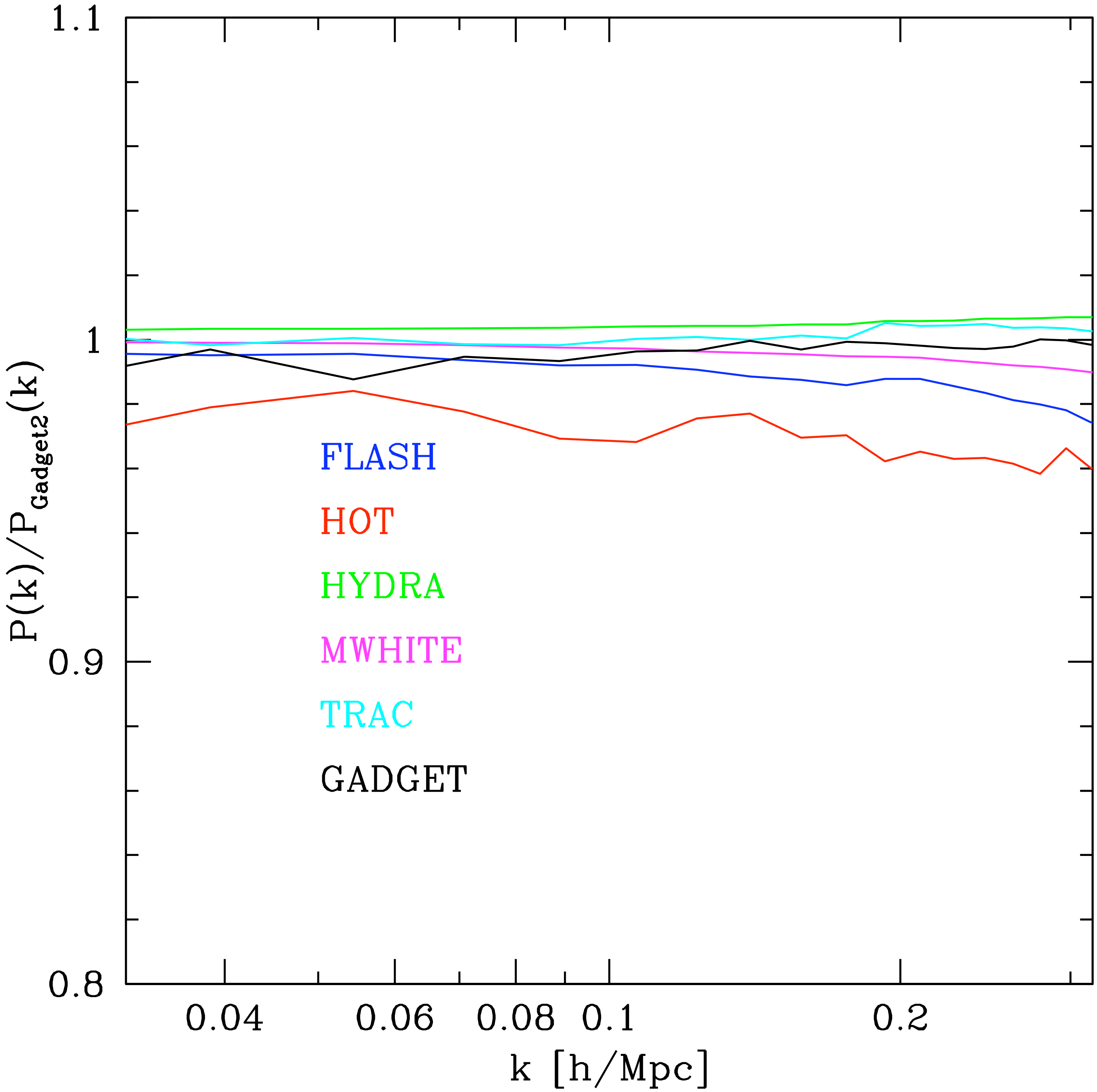

1.1
1
0.9
0.8
0.04
0.06
0.08
0.1
0.2
k [h/Mpc]
P(k)/P_Gadget2(k)
FLASH
HOT
HYDRA
MWHITE
TRAC
GADGET

At present it seems #2 is the most likely explanation. We can guess-estimate the size of the subleading diagrams by recalling that a subset of them renormalizes the power spectrum. Then in the large-k limit we should have

$$G_{ab}(k,\eta) \simeq g_{ab}(\eta)\ \exp\Big(-\frac{1}{2}k^2\sigma_v^2(\mathrm{e}^\eta - 1)^2\Big) \qquad \text{(high-k limit)}$$

with:

$$\sigma_v^2 \equiv \frac{1}{3}\int d^3q \frac{P(q)}{q^2}$$

where P is now replaced by the nonlinear power, instead of linear. This gives a small correction to the exponent in the propagator, making it fall faster.

Recall that the propagator gives the rate of damping of acoustic oscillations, so we want as good a description as possible of it.

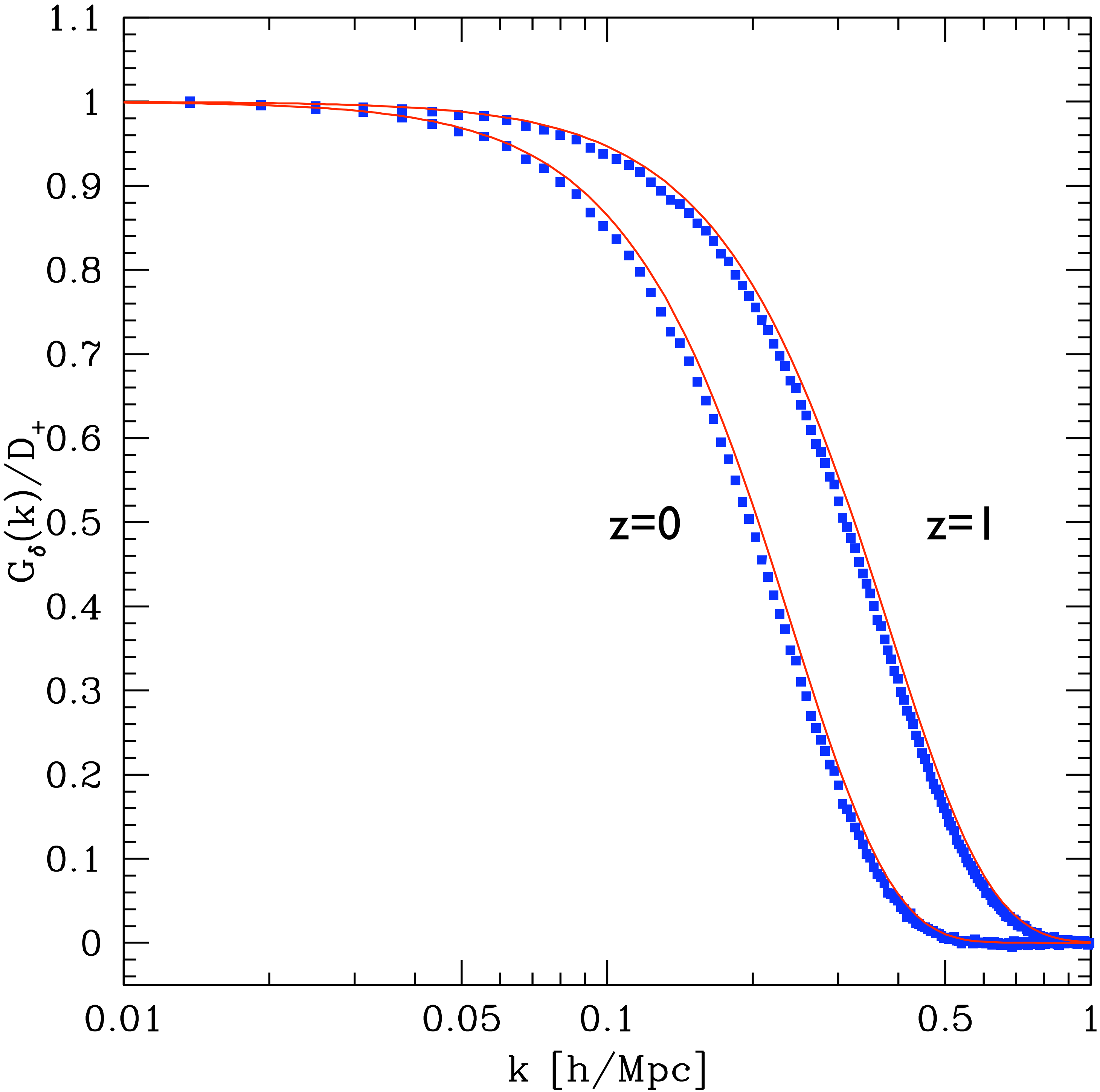

1.1
1
0.9
0.8
0.7
0.6
0.5
0.4
0.3
0.2
0.1
0
$G_\delta(k)/D_+$
z=0
z=1
0.01
0.05
0.1
0.5
1
k [h/Mpc]

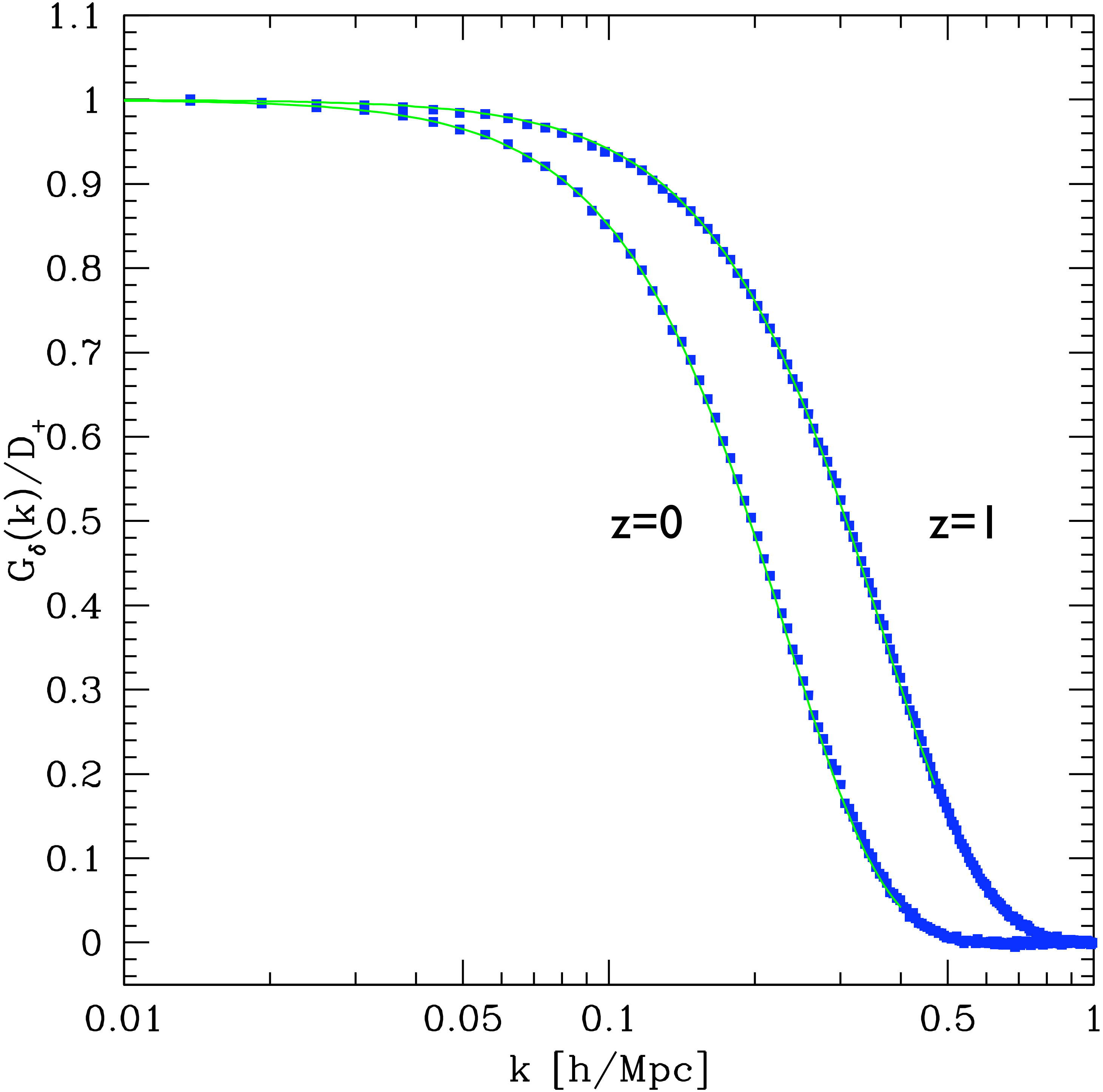

1.1
1
0.9
0.8
0.7
0.6
0.5
0.4
0.3
0.2
0.1
0
$G_\delta(k)/D_+$
z=0
z=1
0.01
0.05
0.1
0.5
1
k [h/Mpc]

Power Spectrum in RPT vs N-Body Simulations

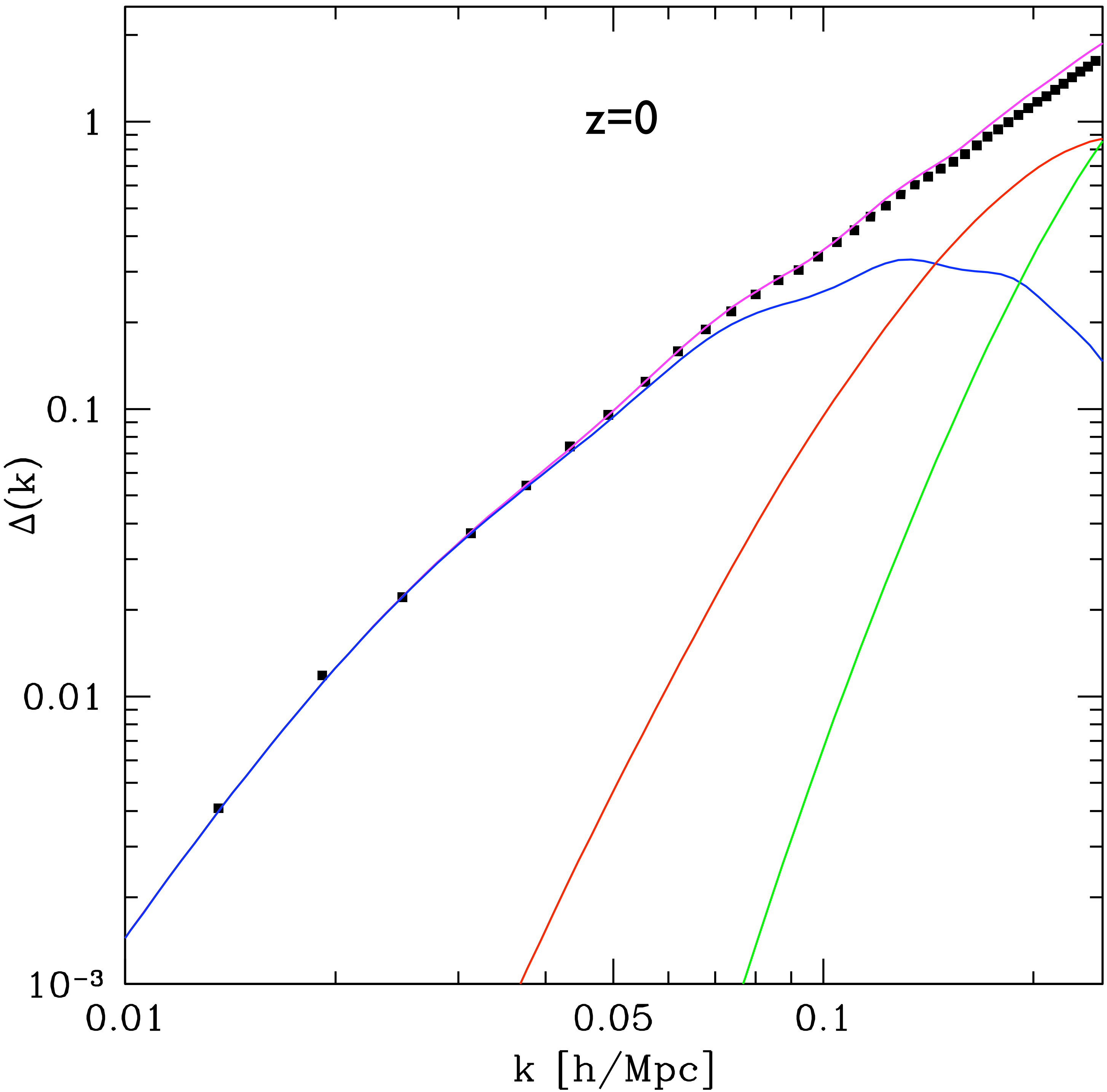

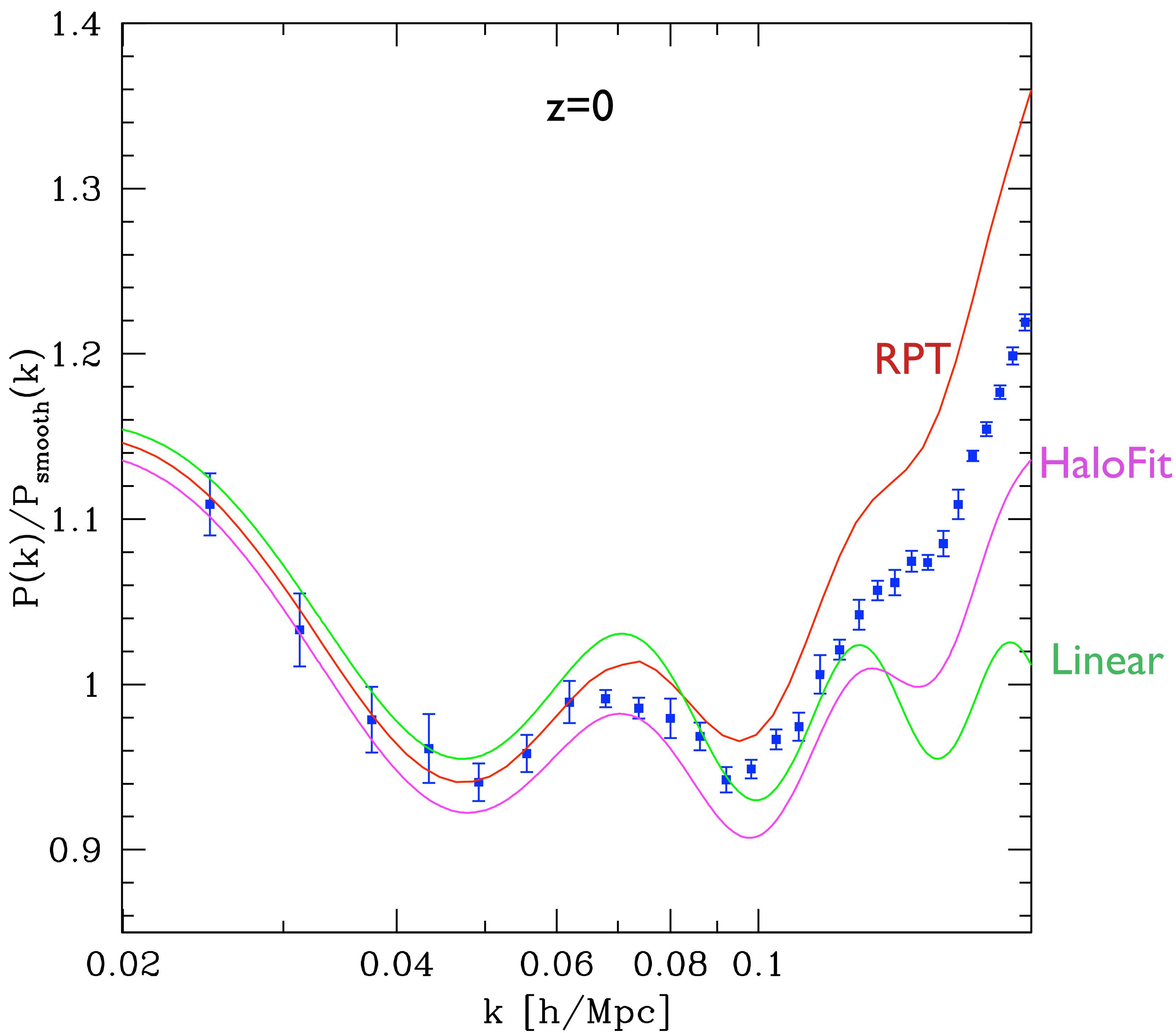
z=0
RPT
HaloFit
Linear
1.4
1.3
1.2
1.1
1
0.9
0.02
0.04
0.06
0.08
0.1
$P(k)/P_{\rm smooth}(k)$
k [h/Mpc]

Corrected propagator automatically gives correct power spectrum

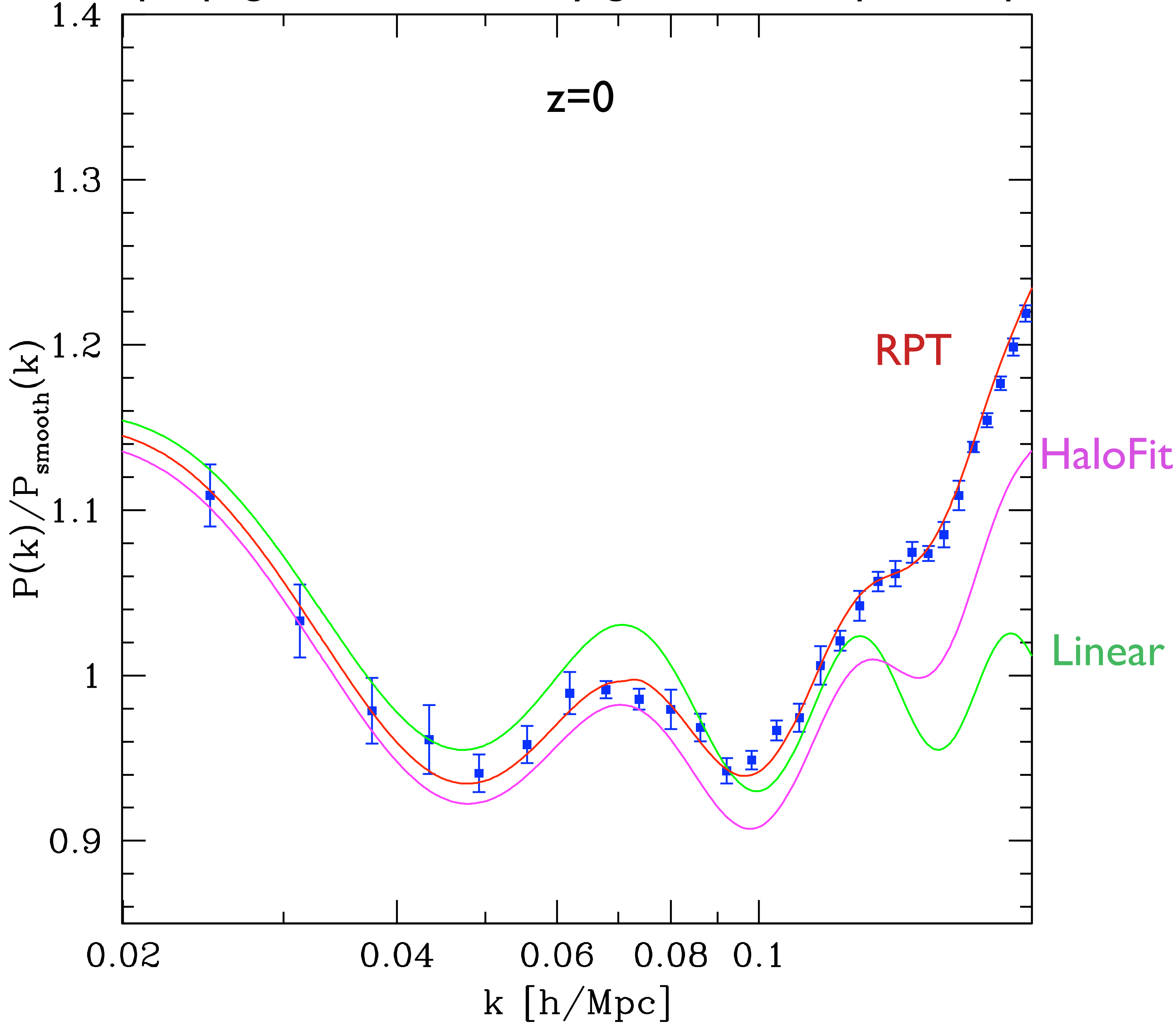

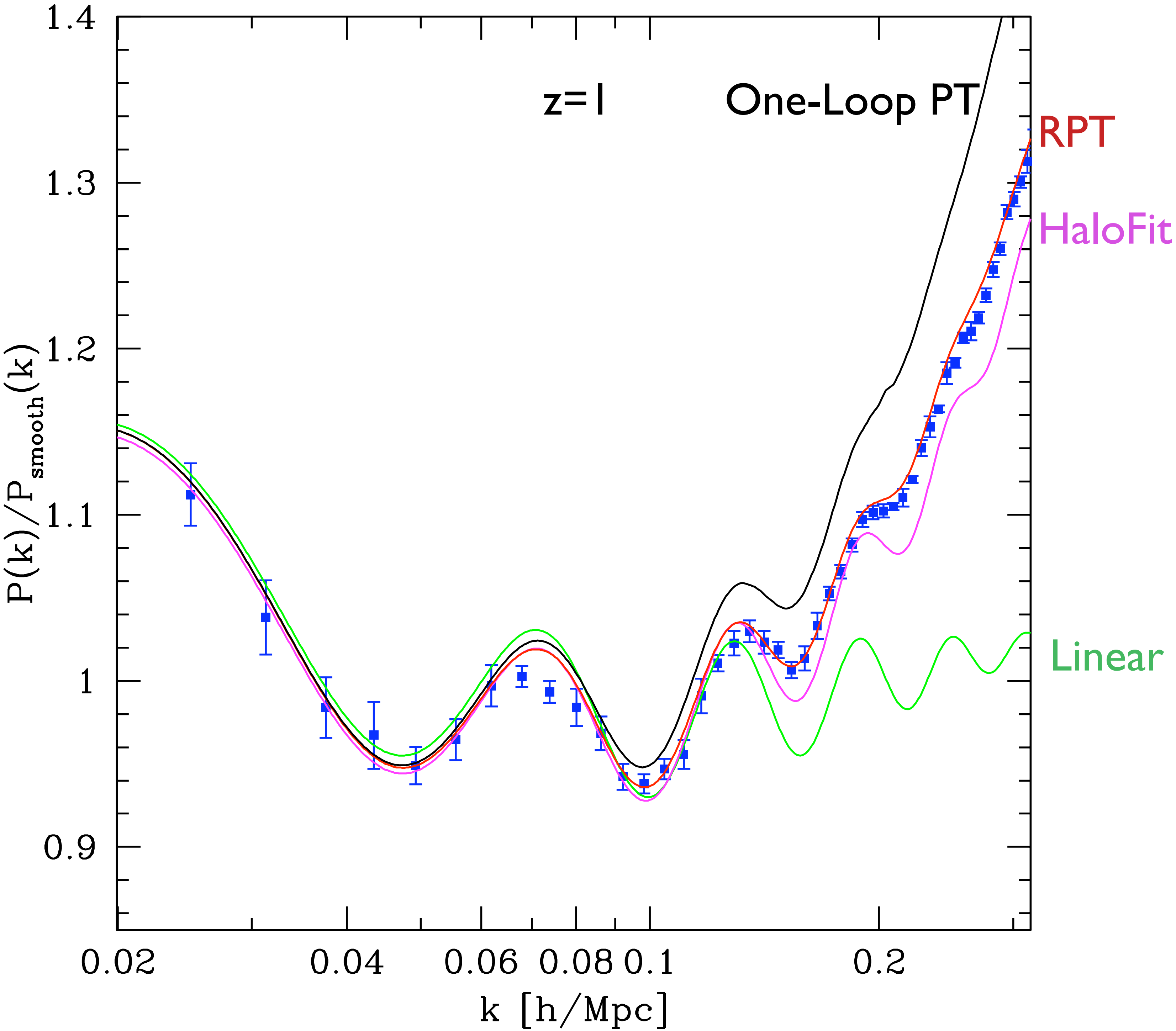

z=1
One-Loop PT
RPT
HaloFit
Linear
$P(k)/P_{smooth}(k)$
k [h/Mpc]
1.4
1.3
1.2
1.1
1
0.9
0.02
0.04
0.06
0.08
0.1
0.2

So far we have discussed dark matter...

Now, let's discuss galaxies, in particular dark matter halos (which are easier to model, and can be populated with galaxies to yield a given galaxy sample).

We are interested in the scale dependence of the bias (clustering), and how it impacts the acoustic oscillations.

The uncertainties are larger here than for dark matter alone. We model halo (and galaxy) clustering using one-loop PT including the effects of nonlinear bias.

The first thing we want to test is the validity of local bias. This says that at large scales the relationship between galaxies (or halos) and dark matter can be approximated by scale-independent bias coefficients,

$$\delta_g \approx b_1 \delta + \frac{b_2}{2!}\delta^2 + \frac{b_3}{3!}\delta^3$$

Fry and Gaztanaga(1993)

Local Bias holds!

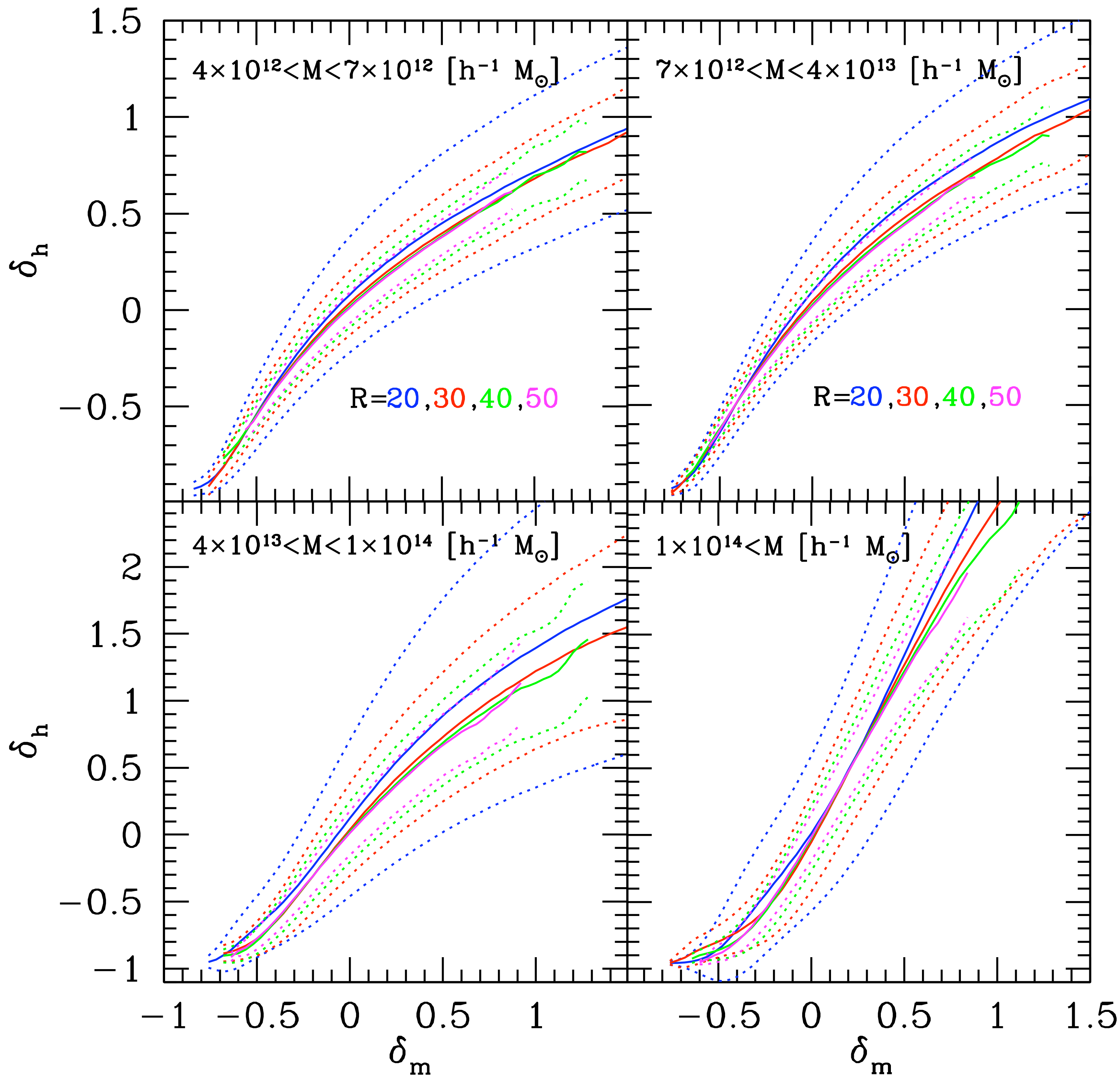

Halo Bias is non-linear: predictions from ST mass function

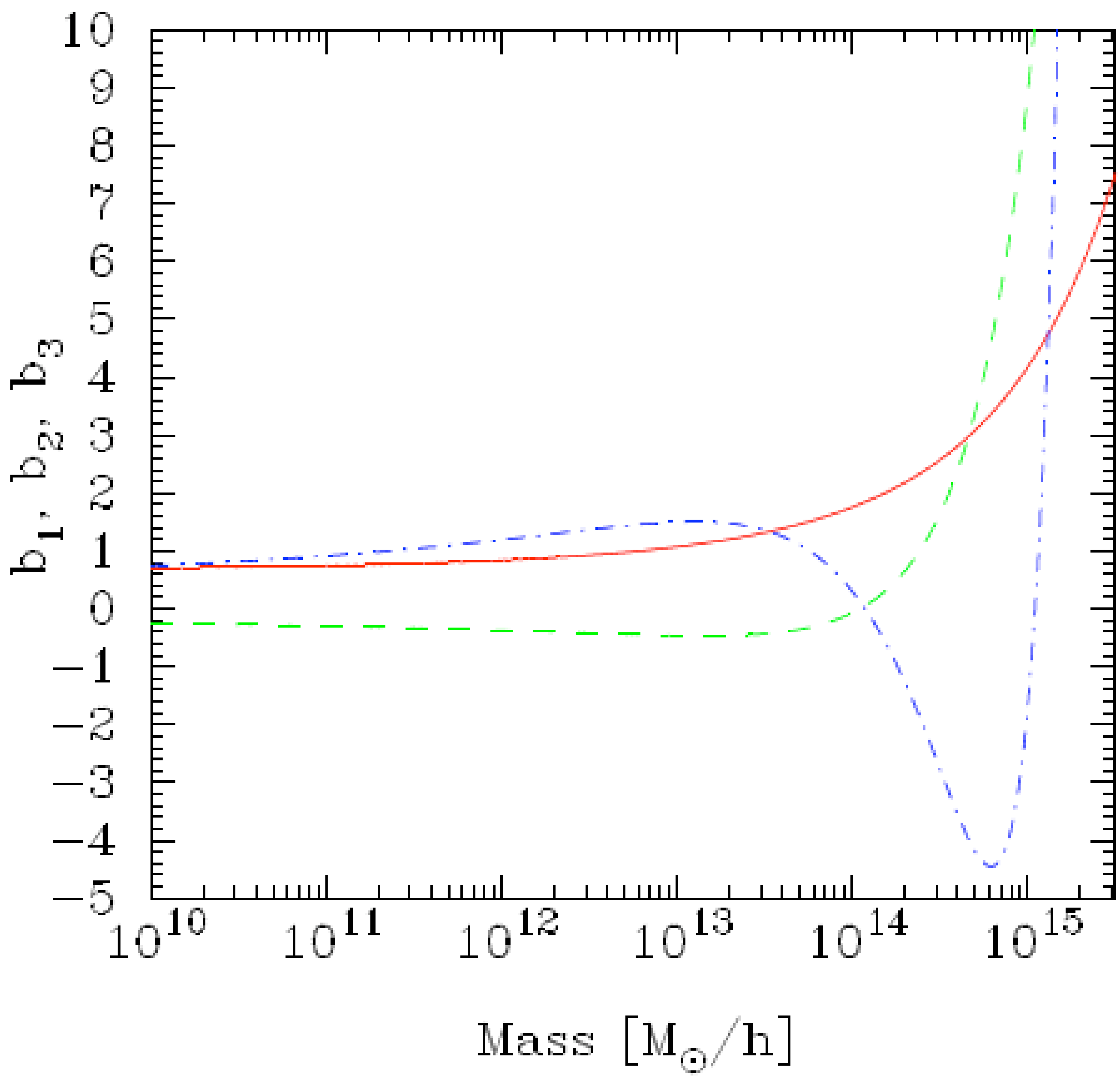

Scoccimarro, Sheth, Hui and Jain (2001)

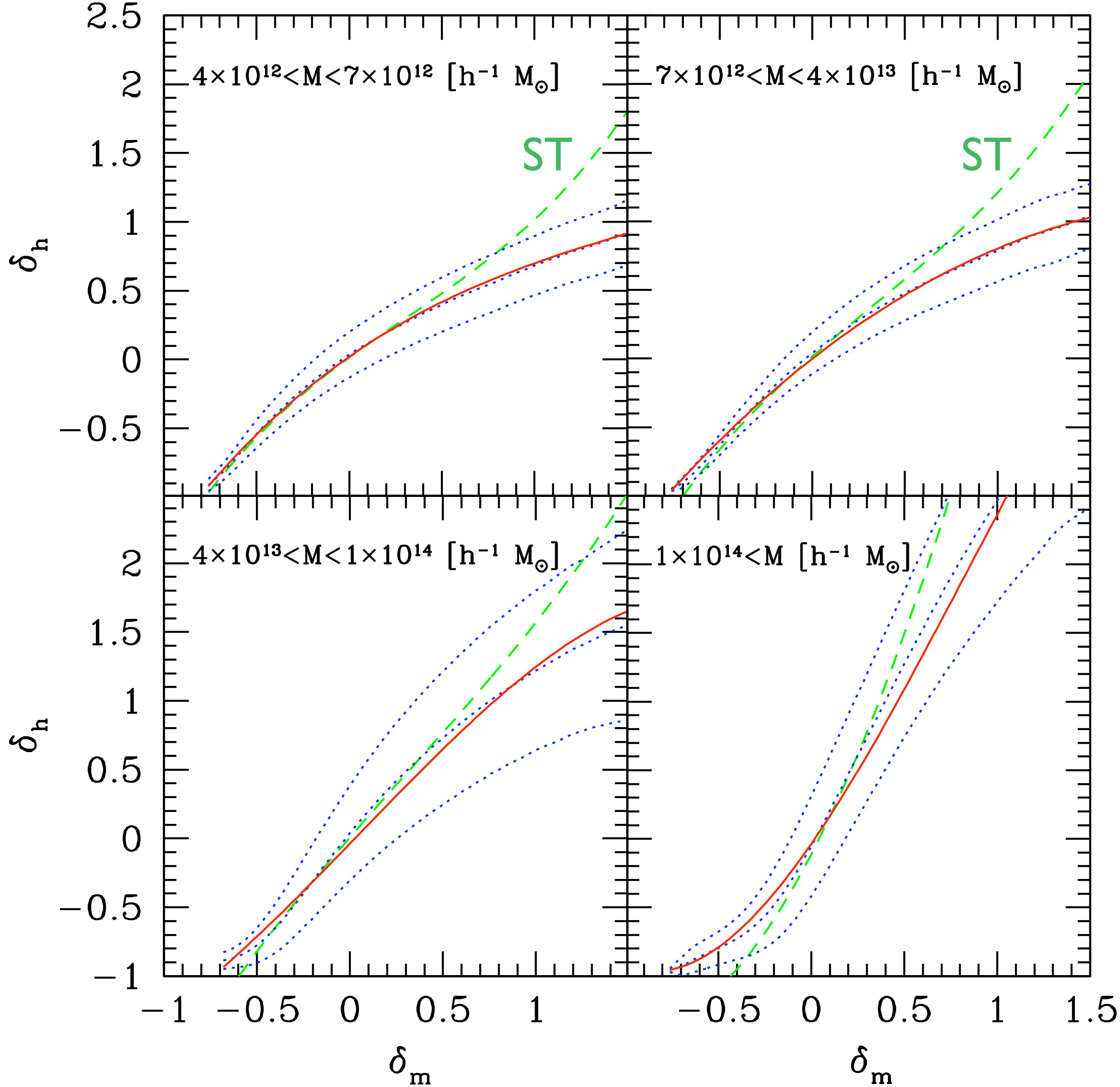

$4\times10^{12}<M<7\times10^{12}$ [h^{-1} $M_\odot$]
ST
$7\times10^{12}<M<4\times10^{13}$ [h^{-1} $M_\odot$]
ST
$4\times10^{13}<M<1\times10^{14}$ [h^{-1} $M_\odot$]
$1\times10^{14}<M$ [h^{-1} $M_\odot$]
δ_h
δ_m
2.5
2
1.5
1
0.5
0
−0.5
−1
−1
−0.5
0
0.5
1
1.5

The effect of nonlinear bias on acoustic oscillations: predictions

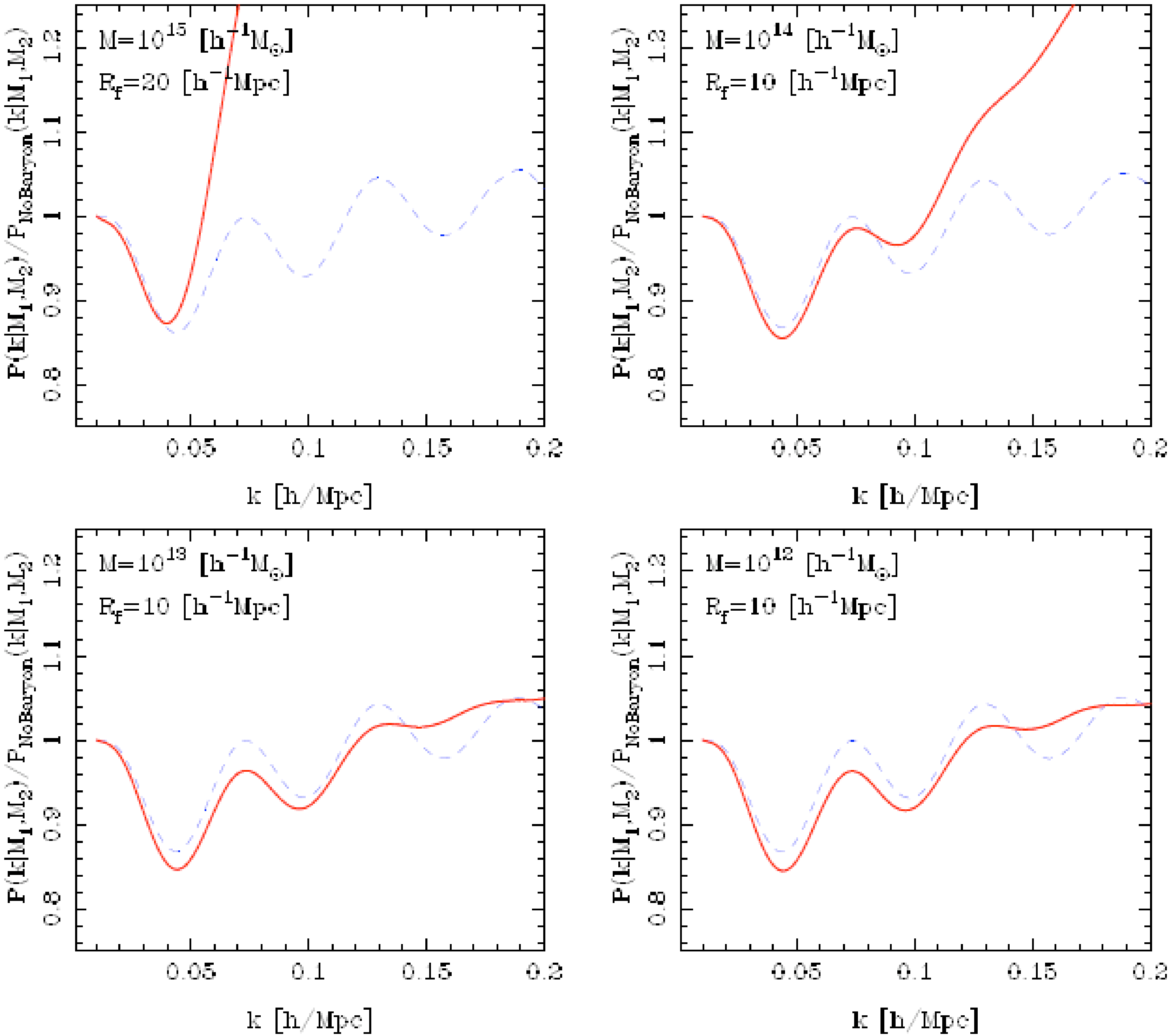

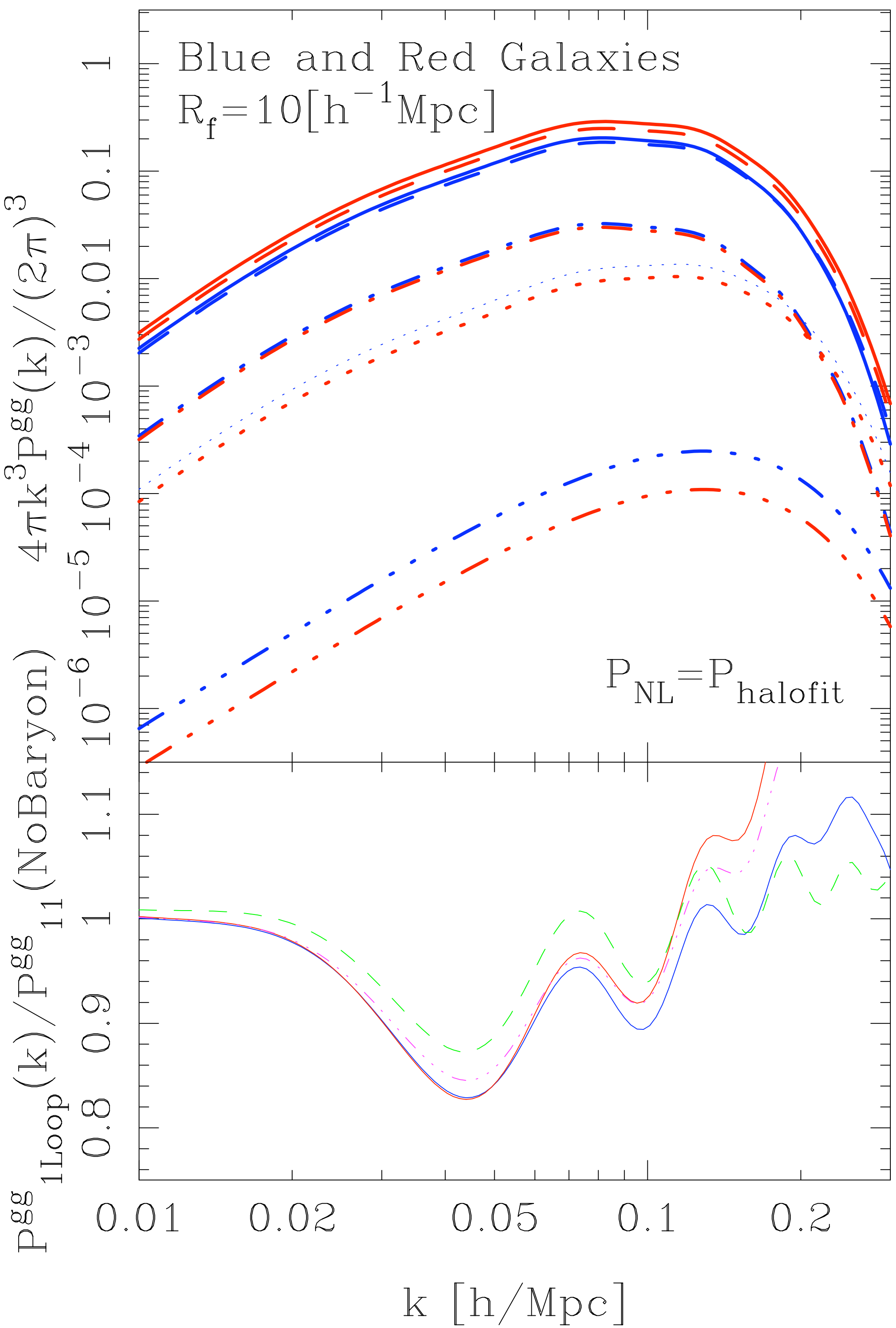

Blue and Red Galaxies
$R_f=10[h^{-1}\mathrm{Mpc}]$
$P_{NL}=P_{halofit}$
$4\pi k^3 P^{gg}(k)/(2\pi)^3$
$P^{gg}_{1Loop}(k)/P^{gg}_{11}$(NoBaryon)
k [h/Mpc]
0.01
0.02
0.05
0.1
0.2
1
0.1
0.01
10^{-3}
10^{-4}
10^{-5}
10^{-6}
1.1
1
0.9
0.8

The effect of nonlinear bias on acoustic oscillations
Comparison with simulations

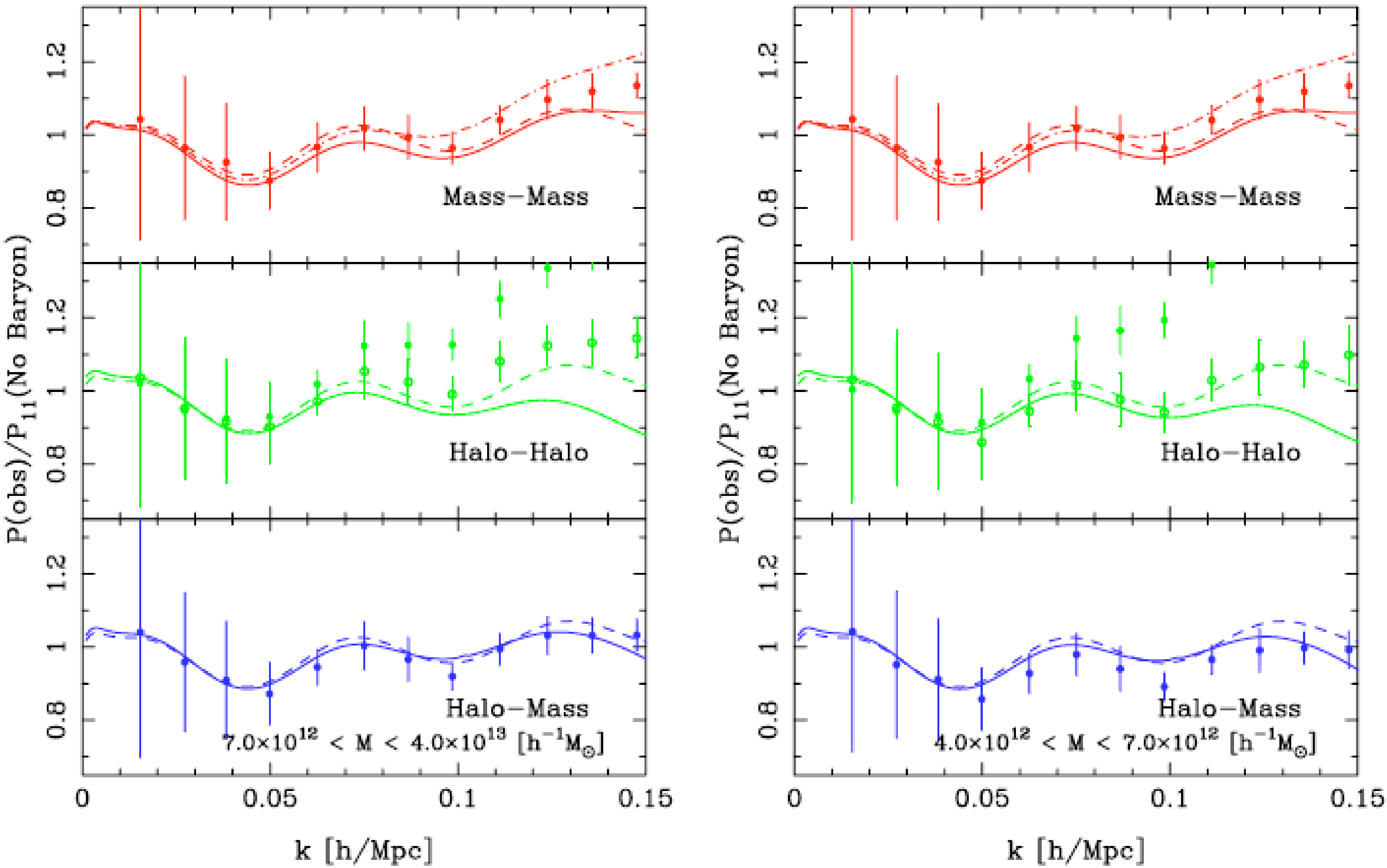

The effect of nonlinear bias on acoustic oscillations
Comparison with simulations

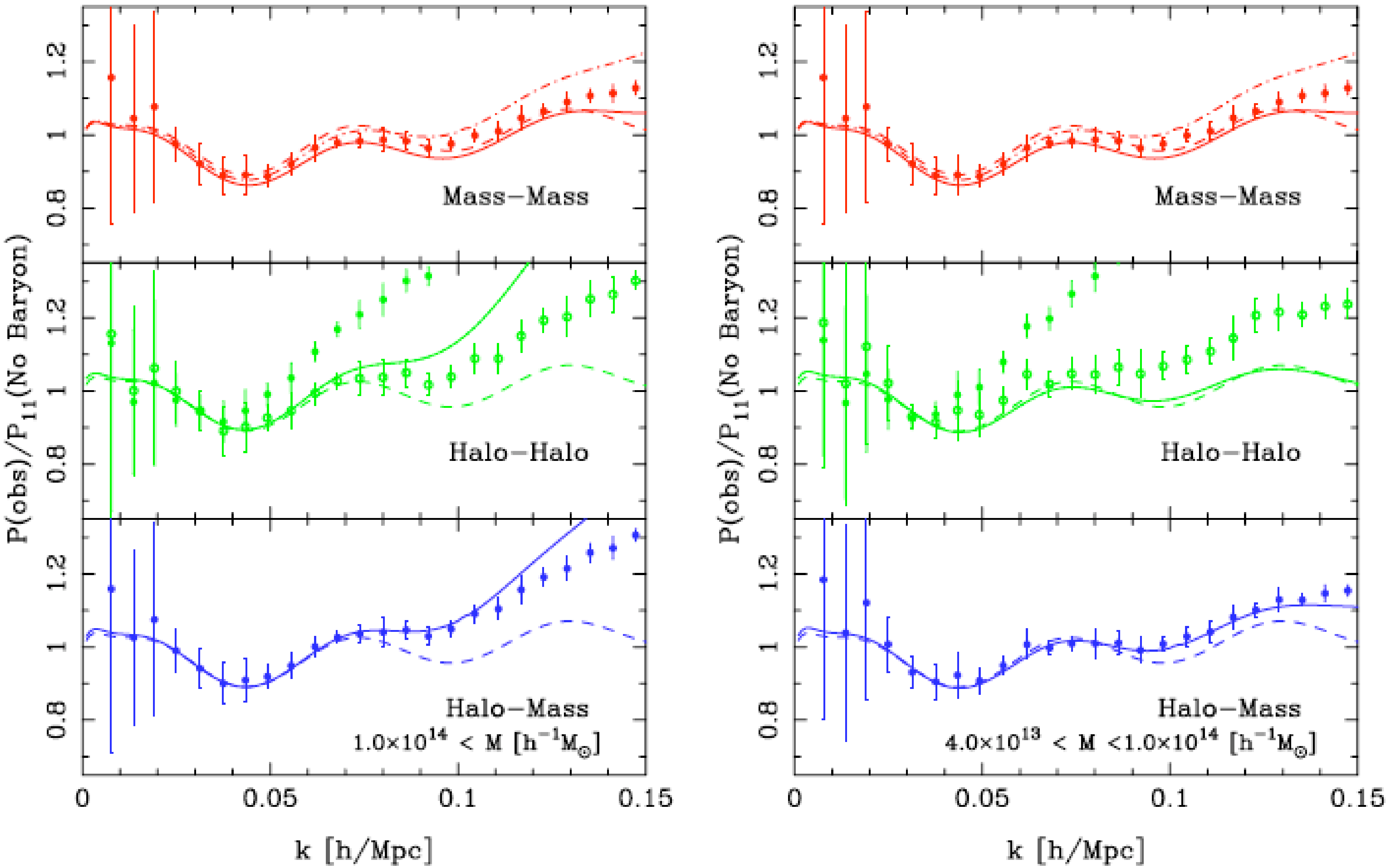

For high halo mass, one must be careful about dealing with sub-Poisson shot noise due to exclusion. In this case, easiest to deal with two-pt function.

The view from the two-pt function...

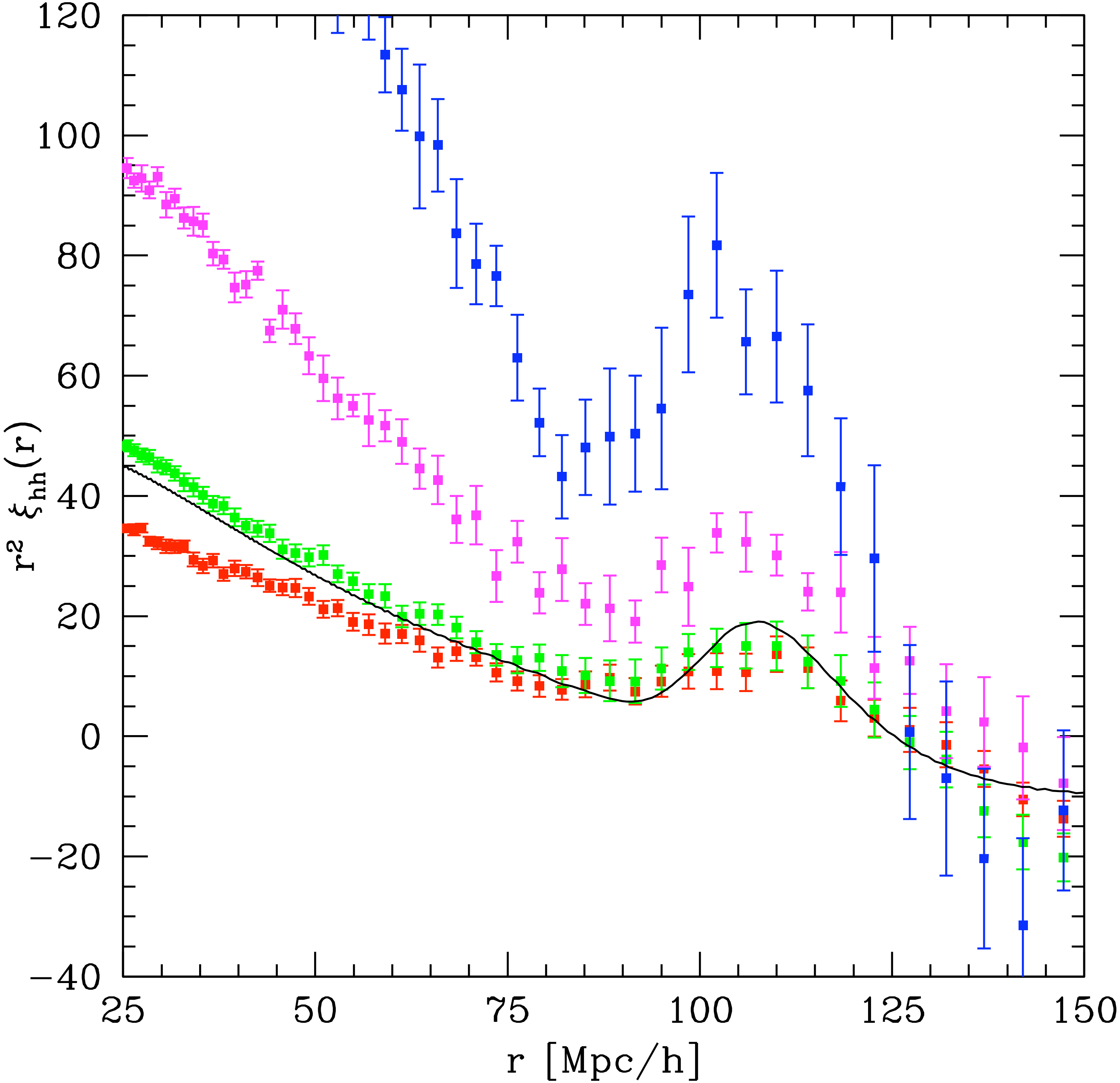

Conclusions and Future Work

- RPT gives a well-behaved perturbation theory. The power spectrum is in excellent agreement with simulations if propagator is modified slightly to match simulations.

- Need to keep an eye on evolution of simulations and code comparison.

- Include redshift-space distortions to see impact on acoustic oscillations.

- Mode-coupling is not strong enough to cause large shifts in the position of acoustic oscillation peaks.

- However, different mass halo populations damp linear waves on progressively larger scales as the halo mass increases. This makes more challenging measuring BAO from the power spectrum of very massive clusters or very luminous galaxies.